VARIABILITY OF K_d VALUES IN CEMENTITIOUS MATERIALS AND SEDIMENTS

P. M. Almond
D. I. Kaplan
E. P. Shine

JANUARY 2012

DISCLAIMER

This work was prepared under an agreement with and funded by the U.S. Government.
Neither the U. S. Government or its employees, nor any of its contractors,
subcontractors or their employees, makes any express or implied:
1. warranty or assumes any legal liability for the accuracy, completeness, or for the use
or results of such use of any information, product, or process disclosed; or
2. representation that such use or results of such use would not infringe privately owned
rights; or
3. endorsement or recommendation of any specifically identified commercial product,
process, or service.
Any views and opinions of authors expressed in this work do not necessarily state or
reflect those of the United States Government, or its contractors, or subcontractors.

Printed in the United States of America

Prepared for
U.S. Department of Energy

VARIABILITY OF K_d VALUES IN CEMENTITIOUS MATERIALS AND SEDIMENTS

P. M. Almond
D. I. Kaplan
E. P. Shine

JANUARY 2012

Savannah River National Laboratory
Savannah River Nuclear Solutions
Savannah River Site
Aiken, SC 29808

Prepared for the U.S. Department of Energy Under
Contract Number DE-AC09-08SR22470

SRNL
SAVANNAH RIVER NATIONAL LABORATORY

TABLE OF CONTENTS

LIST OF FIGURES

LIST OF TABLES

LIST OF ACRONYMS

AD	Analytical Development
AIC	Akaike Information Criterion
AICc	Akaike Information Criterion with correction
BIC	Schwartz's Bayesian information criterion
ARP	Actinide Removal Process
BFS	Blast Furnace Slag
C-H-S	Calcium Silicate Hydrogel (variable $C - S$ ratio)
$Ca(OH)_2$	Portlandite
CSSX	Caustic Side Solvent Extraction
CV	Coefficient of Variation
DI	Deionized
DDA	Deliquification, Dissolution, and Adjustment
DSS	Decontaminated Salt Solution
FA	Fly Ash
K_d	Distribution coefficient
MCU	Modular CSSX Unit
PA	Performance Assessment
OPC	Ordinary Portland Cement
ORP	Oxidation-Reduction Potential
SDF	Saltstone Disposal Facility
SPF	Saltstone Production Facility
SHE	Standard Hydrogen Electrode
SRNL	Savannah River National Laboratory
SRNS	Savannah River Nuclear Solutions
SRS	Savannah River Site
SWPF	Salt Waste Processing Facility

1.0 EXECUTIVE SUMMARY

Measured distribution coefficients (K_d values) for environmental contaminants provide input data for performance assessments (PA) on the Savannah River Site (SRS) that evaluate physical and chemical phenomena for release of radionuclides from wasteforms, degradation of engineered components and subsequent transport of radionuclides through environmental media. This report contains results from two tasks. The first task measured Cs, Sr, I, and Eu K_d values with simulated saltstone. The second task consisted of a critical literature review and statistical analysis of soil Pu K_d values. For both tasks the statistical range and distribution were determined to assist stochastic modelers in site wide PA analyses.

Saltstone K_d Task – The objective of the saltstone K_d variability project was to determine the range and distribution of cesium, strontium, iodine and europium K_d values in saltstone. The scope of this study did not include understanding saltstone sorption mechanisms responsible for increasing or decreasing sorption. Cs, Sr, and I K_d values were measured from a wide range of formulations of 22 archived saltstone materials (measured in triplicate). Eu K_d values could not be measured because Eu precipitated or sorbed to glassware during the experiment. The following K_d ranges, means, and standard deviations were obtained:

- saltstone triplicate Cs K_d values ranged from 5 to 436 mL/g (mean K_d = 20 ± 15 mL/g for <60 °C samples; mean K_d = 289 ± 115 mL/g for 60 °C samples),
- saltstone triplicate Sr K_d values ranged from 122 to 6,938 mL/g (mean K_d = 528 ± 242 mL/g for <60 °C samples; mean K_d = 3383 ± 2401 mL/g for 60 °C samples)
- saltstone triplicate I K_d values ranged from -1.5 to 2.9 mL/g (mean K_d = 1.07 ± 0.97 mL/g for all samples)

The distribution of saltstone K_d values were very wide, capturing the wide array of formulations and temperature curing conditions represented in the samples.

This work suggests keeping the present method of calculating K_d value ranges for stochastic models:

$$\text{``Min''} = K_d - (1.5*0.5*K_d) = 0.25*K_d$$
$$\text{``Max''} = K_d + (1.5*0.5*K_d) = 1.75*K_d$$

This range is not as large as identified experimentally. It is possible that the experimental conditions selected are not in fact those that may prevail in the field. Furthermore, only a small number of samples were analyzed. Two types of distributions were selected for the cementitious materials. Lognormal is used for the cations (Cs, Sr etc…) and the zero-inflated Weibull for the anions that used K_d values including K_d = 0 (e.g. I). The Weibull and lognormal are very common distributions that are available in the GoldSim software presently used on the SRS for stochastic modeling for various PAs.

Soil Pu K_d Task – The range and distribution of plutonium K_d values in soils is not known.   65 SRS sediment Pu-K_d values were critically reviewed, tabulated, and then statistically analyzed to identify their range and distributions, similar to what was done with the saltstone K_d values. Further refinement of the distributions was made based on the soil texture and soil pH range. The purpose of the Pu sediment K_d dataset was not to attempt to understand through statistics how to better understand Pu sorption to sediments or to lower Pu K_d variance. The following K_d ranges, means, and standard deviations were obtained:

- pH 4.6 to 10.47 sediment Pu K_d values ranged from 100 to 50,000 mL/g (mean K_d = 8,559 ± 10,823 mL/g; to simulate a plume moving through all pH conditions),
- pH 4.6 to 7.0 sediment Pu K_d values ranged from 100-33,000 mL/g (mean = 6,047 ± 6,971 mL/g ; to simulate a plume moving through far-field conditions),
- pH 7.01 to 10.47 sediment Pu K_d values ranged from 210 – 50,000 mL/g (mean = 12,851 ± 14,525 mL/g; to simulate a plume moving through a basic cementitious plume conditions), and

The Weibull distribution was recommended for each of the Pu sediment distributions. The large range in Pu K_d was a result of a sharp rise or drop in K_d values, consequently, if the intent is to reduce the range of K_d values, then smaller ranges of pH values are recommended. The recommended best estimate Pu K_d value for sandy sediments was increased from 290 to 650 mL/g based on long-term field lysimeter studies, and the observation that the 290 mL/g value was within the 10-25 percentile of Pu K_d values in sandy sediments.

2.0 INTRODUCTION

Measured distribution coefficients (K_d values) for environmental contaminants provide input data for performance assessments (PA) that evaluate physical and chemical phenomena for release of radionuclides from wasteforms, degradation of engineered components and subsequent transport of radionuclides through environmental media. Research efforts at SRNL to study the effects of formulation and curing variability on the physiochemical properties of the saltstone wasteform produced at the Saltstone Disposal Facility (SDF) are ongoing and provide information for the PA and Saltstone Operations. Furthermore, the range and distribution of plutonium K_d values in soils is not known. Knowledge of these parameters is needed to provide guidance for stochastic modeling in the PA.

Under the current SRS liquid waste processing system, supernate from F & H Tank Farm tanks is processed to remove actinides and fission products, resulting in a low-curie Decontaminated Salt Solution (DSS). At the Saltstone Production Facility (SPF), DSS is mixed with premix, comprised of blast furnace slag (BFS), Class F fly ash (FA), and portland cement (OPC) to form a grout mixture. The fresh grout is subsequently placed in SDF vaults where it cures through hydration reactions to produce saltstone, a hardened monolithic waste form.

Variation in saltstone composition and cure conditions of grout can affect the saltstone's physiochemical properties. Variations in properties may originate from variables in DSS, premix, and water to premix ratio, grout mixing, placing, and curing conditions including time and temperature (Harbour et al. 2007; Harbour et al. 2009).

There are no previous studies reported in the literature regarding the range and distribution of K_d values in cementitious materials. Presently, the Savannah River Site (SRS) estimate ranges and distributions of K_d values based on measurements of K_d values made in sandy SRS sediments (Kaplan 2010). The actual cementitious material K_d values and solubility values differ from the sandy sediments. The K_d value range and distribution currently used in the PA are estimated to range between $0.25*K_d$ and $1.75*K_d$, where the minimum and maximum values of the ranges reflect the 95% confidence level for the mean K_d value (Kaplan 2010).

The objective of the research with cementitious materials was to measure the range and distribution of a monovalent (Cs) and I^- (anion), divalent (Sr), and trivalent (Eu) ions for a variety of laboratory-prepared saltstone surrogate samples to establish a K_d range other than that which is presently used in the PA. It has been observed in laboratory samples that cure temperature profiles can affect properties such as heat of hydration, permeability, porosity, compressive strength, and set time (Harbour et al. 2009). The intent was to identify a range and distribution that could be used by stochastic modelers for the PA. Furthermore, the intent was to replace the arbitrarily selected distributions based on geological sandy sediments and to base it on actual cementitious materials. The scope of this study did not include understanding saltstone sorption mechanisms responsible for increasing or decreasing sorption.

Similar to the work with cementitious materials, the purpose of the Pu sediment K_d dataset was not to attempt to understand through statistics how to better understand Pu sorption to sediments

or to lower Pu K_d variance.   The sediment Pu K_d data is included in this study because it is a key risk driver for the PAs on the SRS, and there is presently no direct studies of Pu variability in SRS soils. Instead the distribution of Pu sediment K_d values was assumed to be similar to other cations, as presented by Kaplan (2010).

3.0 EXPERIMENTAL

3.1 SAMPLE SELECTION AND CHARACTERIZATION - CEMENTITIOUS SAMPLES

Twenty-two unique cementitious samples were selected from hundreds of archived samples that were prepared between 2008 to 2011 as part of Saltstone Variability studies and have relevance to saltstone performance (Table 1). Archived samples were initially inventoried to identify availability of the samples. Information from all located samples was compiled and was subsequently down selected to twenty-two to be used for experiment. The samples contained variation in their composition and preparation conditions, and these variables included, initial cure temperature profile, premix ratio, water to premix ratio, simulant solution, aluminate concentration, and sample age (Table 1, Table 3). The samples had been archived in labeled plastic bags or a capped plastic molds. Sample information was available in SRNL laboratory notebooks (Grout Variability Study 1-7) and SRNL reports (Harbour 2008, 2009).

Table 1. Samples selected for K_d variability study and key variables.

Sample Identification [1]	Simulant[2]	Premix Ratio (FA/Slag/OPC)	Water to Premix Ratio	Aluminate Concentration	Max Controlled Cure Temp (°C)[3]	Sample Age (Years)
GVS-88	SWPF	45/45/10	0.60	0.11	60	2.9
GVS-93	SWPF	30/60/10[3]	0.60	0.45	22	2.9
GVS-94	SWPF	45/45/10	0.60	0.45	22	2.9
GVS-100-01	SWPF	45/45/10	0.60	0.28	22	2.8
GVS-100-02	SWPF	45/45/10	0.60	0.28	60	2.8
GVS-107	MCU	45/45/10	0.60	0.05	22	2.6
GVS-110	MCU	45/45/10	0.59	0.22	22	2.6
GVS-111	MCU	45/45/10	0.64	0.22	22	2.6
GVS-114	MCU	30/60/10	0.59	0.22	22	2.6
GVS-118	MCU	25/45/30	0.60	0.22	22	2.5
GVS-121	SWPF	45/45/10	0.60	0.35	22	2.2
GVS-123	SWPF	45/45/10	0.60	0.55	22	2.2
TR-419	MCU	45/45/10	0.60	0.05	22	3.7
TR-503	MCU	45/45/10	0.50	0.05	22	3.1
TR-513	SWPF	45/45/10	0.45	0.11	22	3.0
TR-517	MCU	45/45/10	0.60	0.05	40	3.0
TR-531	DDA	45/45/10	0.60	0.07	22	3.0
TR-614	MCU	25/45/30	0.60	0.22	22	2.2
TR-616	MCU	45/45/10	0.55	0.22	40	2.2
TP-006-003	Tank 50	45/45/10	0.55	0.28	41	0.8
TP-006-004	Tank 50	45/45/10	0.55	0.28	48	0.8
TP-006-005	Tank 50	45/45/10	0.55	0.28	57	0.8

[1]Similar samples are grouped together by white or gray shading.
[2]See Table 2 for simulant composition for each sample.
[3]22 °C represents ambient laboratory temperature.

Table 2. Simulant components and concentrations (Molarity) for selected samples.

Sample Identification	Simulant[2]	50 wt% NaOH	NaNO$_3$	NaNO$_2$	Na$_2$CO$_3$	Na$_2$SO$_4$	Aluminum Nitrate (9 H$_2$O)	Sodium Phosphate (12 H$_2$O)
DDA-PA[1]	DDA	0.769	2.202	0.110	0.145	0.044	0.071	0.008
MCU-PA[1]	MCU	1.594	3.159	0.368	0.176	0.059	0.054	0.012
SWPF-PA[1]	SWPF	2.866	1.973	0.485	0.118	0.055	0.114	0.007
GVS-88	SWPF	2.368	2.374	0.580	0.118	0.055	0.114	0.007
GVS-93	SWPF	4.705	1.371	0.583	0.118	0.055	0.449	0.007
GVS-94	SWPF	3.705	0.568	0.386	0.118	0.055	0.449	0.007
GVS-100-01	SWPF	3.535	1.128	0.484	0.118	0.055	0.282	0.007
GVS-100-02	SWPF	3.535	1.128	0.484	0.118	0.055	0.282	0.007
GVS-107	MCU	2.000	1.700	0.550	0.176	0.059	0.220	0.012
GVS-110	MCU	2.680	1.700	0.550	0.176	0.059	0.220	0.012
GVS-111	MCU	2.680	1.700	0.550	0.176	0.059	0.220	0.012
GVS-114	MCU	2.680	1.700	0.550	0.176	0.059	0.220	0.012
GVS-118	MCU	2.680	1.700	0.550	0.176	0.059	0.220	0.012
GVS-121	SWPF	3.810	NA	NA	0.118	NA	0.350	0.007
GVS-123	SWPF	4.610	NA	NA	0.118	NA	0.550	0.007
TR-419	MCU	1.594	3.159	0.368	0.176	0.059	0.540	0.012
TR-503	MCU	1.594	3.159	0.368	0.176	0.059	0.540	0.012
TR-513[1]	SWPF	2.866	1.973	0.485	0.118	0.055	0.114	0.007
TR-517	MCU	1.594	3.159	0.368	0.176	0.059	0.540	0.012
TR-531[1]	DDA	0.769	2.202	0.110	0.145	0.044	0.071	0.008
TR-614	MCU	2.680	1.700	0.550	0.176	0.059	0.220	0.024
TR-616	MCU	2.680	1.700	0.550	0.176	0.059	0.220	0.024
TP-006-003	Tank 50	2.920	1.520	0.550	0.176	0.059	0.280	0.012
TP-006-004	Tank 50	2.920	1.520	0.550	0.176	0.059	0.280	0.012
TP-006-005	Tank 50	2.920	1.520	0.550	0.176	0.059	0.280	0.012

[1]Assumed PA projection (NB Grout Variability # 5 page 83)
[2]Variations of SWPF, MCU, or DDA simulant.

Table 3. Sample heating profiles.

Sample Identification[1]	Max Controlled Cure Temp	Heating Profile
GVS-88	60 °C	Isothermal at 60 °C for 1 day
GVS-100-02	60 °C	Isothermal at 60 °C for 28 days
TR-517	40 °C	Isothermal at 40 °C for 7 days
TR-616	40 °C	Isothermal at 40 °C for 1 day
TP-006-003	41 °C	Ramped to 41.1 °C over 3 days
TP-006-004	48 °C	Ramped to 47.9 °C over 4 days
TP-006-005	57 °C	Ramped to 56.4 °C over 5 days

Sorption experiments were performed in air to acquire distribution coefficients (K_d) for the measurable elements present in the solid and aqueous leachate at equilibrium. Approximately 0.5 grams of the sample were ground using a mortar and pestle and then added to 7 mL of a saturated $Ca(OH)_2$ solution for each leaching experiment. Leach solutions were contacted with the solid for 7 or more days (7-26 d) and subsequently filtered using a 0.45 μm filter.

K_d values (mL/g) were calculated from measurements of the quantity of material in the solids and the quantity of material in the liquids.

$$K_d = \frac{(C_i - C_f) \times V}{C_f \times m_{solids}}$$

(1)

where Ci is the aqueous activities of the initial (from the "no solids" controls) and Cf is the final equilibrium activity of each radionuclide (dpm/mL); V = volume of liquid in the final equilibrated suspension (mL); and msolids is the solids mass (g). C_i and C_f values of the gamma emitting radionuclides.

A Portlandite ($Ca(OH)_2$) saturated leaching solution was used in the desorption tests to simulate young and moderately aged cementitious materials[1], defined in Kaplan 2010. During this cement aging stage, $Ca(OH)_2$ and calcium-silicate-hydrate gels are the key solid phases controlling aqueous leachate chemistry (Berner 1992), because CO_2 in air is very soluble in water at high pH, the resulting dissolved carbonate (CO_3^{2-}) will precipitate as calcite ($CaCO_3$) in the $Ca(OH)_2$ saturated solution. The pH of a $Ca(OH)_2$ saturated solution is approximately 12.5. Deionized (DI) water was used for the preparation of $Ca(OH)_2$-saturated solutions. Approximately 20 g of reagent grade $Ca(OH)_2$ was added to 2 liters of DI water and stirred for one day. The solution was subsequently filtered using a 0.45 μm filter.

3.2 MATERIALS AND METHODS

Saltstone samples were made with simulants of non-radioactive solutions based on projections at the time of DDA, MCU, and SWPF DSS, and Tank 50 analysis (Table 1). Recipes and formulations are presented in detail in Appendix A. Premix was acquired as part of a delivery of cementitious materials to Saltstone used at the SDF (Harbour et al. 2009).

The following is a brief description of the materials and methods used to obtain K_d values for the cementitious materials measured in air.

---

[1] The age of the cementitious material varies with the number of pore volumes that passes through the material and "ages" the material (Berner 1992). "Young cementitious materials" may last 1 to 100 pore volumes. In the past, PAs have assumed 50 pore volumes. They have mineral assemblages that produce a aqueous pH of>12, Moderately aged cementitious solids, produce a aqueous phase of pH ~12 and lasts between 100 and 1000 pore volumes. Kaplan 2010 made calculations demonstrating cementitious materials longevity of this stage lasted 500 pore volumes. The third and final cementitious age can last between 1000 and 10,000 pore volumes

3.2.1 Materials - Cementitious Materials

- Archived cementitious samples.
- Portlandite (Ca(OH)$_2$) saturated leaching solution
- ^{137}Cs, ^{85}Sr, ^{152}Eu, and ^{129}I isotopes
- Hammer and chisel
- Mortar and pestle
- Test tube rotisserie
- pH
- and ORP meter

3.2.2 Methods - Cementitious Materials

Saltstone Samples: Twenty-two 10 g subsamples were collected from various existing simulant saltstone samples that reflect variable formulations, some of which may exist or could be expected to exist in the Saltstone facility. Samples were selected based on availability in an effort to obtain a range of saltstone compositions.

Batch Test: Conduct batch tests with ground cementitious samples, three replicates, nominally 0.5 g saltstone: 7 mL saturated Ca(OH)$_2$ on the lab bench (or hood). Leach solutions containing radionuclide isotopes were in contact with cementitious material for at least a 7 day contact period. Samples were filtered using a 0.45 μm filter and subsequently analyzed by gamma spectroscopy to determine equilibrium solution concentrations. 'No solids control' samples were analyzed to determine initial solution concentrations for experiments with cementitious materials.

A Portlandite saturated leaching solution was prepared for use in the desorption tests to simulate young/moderately aged cement pore solution (Kaplan et al. 2008). DI water was used for the preparation of Ca(OH)$_2$-saturated solutions. Approximately 20 g of reagent grade Ca(OH)$_2$ was added to2 liters of DI water and stirred for one day. The solution was subsequently filtered using a 0.45 μm filter.

All tests were conducted in triplicate. A positive control was included with each set of experiments; "no-solids" control samples were used to determine if precipitation of the radionuclides occurred during the experiments. K$_d$ values of Cs, Sr, and I were calculated using Equation 1, which calculates sorption by subtracting the concentration of radionuclide added from the concentration remaining in solution at the end of the one-week or greater equilibration period..All AD data is archived in the Analytical Development's LIMS system.

To set up the leaching experiments, nominally 0.5 g amounts of the ground cementitious materials were each added to a clean 15 mL centrifuge tube for each test, and labeled with the identification of the sample. Experiments were run in triplicate. The solution phase was held constant for all sorption experiments and contacted with the solids for 7- 28 days. For each experiment, centrifuge tube was continuously rotated on a rotisserie during the contact period. The solutions were subsequently filtered using a 0.45 μm filter. Approximately 4 mL of each

solution was submitted to AD for analysis of final radionuclide concentration. The initial spike concentration was determined by using the data from the no-solids control sample.

3.2.3 Materials and Methods - Soil Samples

Selection of Sediment Pu K_d Values from the Literature: Selection of Pu K_d values from the literature had to meet the following criteria; that is they had to be measured in:

- SRS sediment,
- In pH 4.6 to 7.0,
- Been spiked with Pu(IV) or Pu(V)
- If spiked with Pu(V), the Pu(V) had to have contact with the soil greater than 2 days (to permit Pu(V) reduction to Pu(IV) (Kaplan, 2006) (Powell, 2002a)). This minimum of two days of contact time was selected based on careful oxidation state characterization experimentation and approach to equilibration experimentation conducted on SRS sediments (Kaplan et al., 2004; Powell, 2002b). In short, once Pu(V) comes in contact with SRS sediments, even under bench top conditions, it undergoes near complete reduction to Pu(IV) within 30 hr; Pu(V) concentration decrease and ingrowth of Pu(IV) increases in the aqueous phase and solid phase. After one day of contact, Pu(V) K_d values were one to three orders of magnitude lower than Pu(IV) K_d values added to the same sediment.   Within 33 days, K_d values of the Pu(V) spiked samples had increased to the same levels as those of the Pu(IV) spiked samples. Some of these kinetic oxidation transformation trends and approach to steady state conditions are demonstrated in the data presented in Appendix B.

Furthermore, to estimate the range and distribution of K_d values in a cementitious leachate passing through sediment the above selection criteria were used, except:

- the acceptable pH criteria were expanded to 4.6 to 11.0.

 The average pH of SRS aquifer groundwater is ~5.5 (Kaplan, 2010).

The soil type, pH, K_d, Pu contact time, reference, and oxidation state of the Pu spike are presented in Table 12. Pu Kd values selected from the literature used to develop the Pu Kd sediment distribution (sorted by pH). The properties of the sediments used in the Pu K_d measurements selected are presented in Table 13.

3.2.4 Statistical Approach – Distribution Model Comparisons

Eleven different models were evaluated for their ability to fit the K_d value distributions. They included the Frechet, generalized Gamma, loglogistic, lognormal, log Generalized Gamma, Weibull, Exponential, LEV, logistic, Normal, and SEV; they are defined in the software JMP (SAS Cary, NC). The approach for selecting the appropriate distribution model was to first do statistical analyses through the use of three goodness-of-fit test: AIC: Akaike information criterion; BIC: Schwartz's Bayesian information criterion; -2 log likelihood: -2 times the natural

log of the likelihood evaluated with the best-fit estimates of the parameters). One can obtain a rather simple and quick understanding of these parameters through a WIKIPEDIA search of "Akaike information criterion" and a more detailed description can be found in Claeskens and Hjort (2008). Each of these goodness-of-fit tests provided slightly different information about how well the estimated distribution models fit the actual K_d distributions, i.e., they are tools for model selection, they rank models.[2] Then the actual distributions were plotted and they were inspected to make sure that the *general* fit that was represented by the goodness-of-fit, capture the more salient aspects of the dataset, including the low K_d as well as the high K_d values (as opposed, for example, only capturing the midrange- and high- K_d data). The goodness-of-fit provides a measure that is appropriate for ranking however it does not tell you if the fit is adequate for a specific application. Then finally, we evaluated whether there was a consistency with a given distribution model, suggesting that a general consistency may exist through a phenomenological process in the data set. The intent was to assign as few distributions as possible and if multiple distributions are assigned, assign them with different populations in mind. The stochastic modeling conducted in Goldsim includes an entire distribution, which include 2σ or 95% confidence.

4.0 RESULTS AND DISCUSSION

K_d values include not only adsorption and absorption mechanisms, but can also reflect precipitation. Some precipitation of the radionuclides may have occurred because control samples where aqueous radionuclide concentration decreases were observed in the absence of added solids. Precipitation or adsorption to test vessel walls of Eu precluded the ability to calculate K_d values. Eu concentrations were below detection limits for no-solid controls and all samples containing cementitious solids. Therefore the measured decreases in aqueous radionuclides were due to causes other than the sorption of the radionuclides by the added solid phases.

In Table 4 calculated K_d values are presented for Cs, Sr, and I for each replicate (A, B, C) and the average of the three replicates. A discussion of results by element follows.

---

[2] As a rough rule of thumb, models having their AIC within 1–2 of the minimum have substantial support and should receive consideration in making inferences. Models having their AIC within about 4–7 of the minimum have considerably less support, while models with their AIC > 10 above the minimum have either essentially no support and might be omitted from further consideration or at least fail to explain some substantial structural variation in the data - Akaike, Hirotsugu (1980). "Likelihood and the Bayes procedure", *Bayesian Statistics*, Ed. J. M. Bernardo *et al.*, Valencia: University Press. p.143-166.

Table 4 . K$_d$ values (mL/g) calculated from adsorption experiments for cesium, strontium, and iodine.

Sample ID	Cesium (K$_d$)				Strontium (K$_d$)				Iodine (K$_d$)			
	A	B	C	Average K$_d$ (ABC)	A	B	C	Average K$_d$ (ABC)	D	E	F	Average K$_d$ (DEF)
GVS-88	436	310	363	370	4801	3501	6938	5080	0.8	-0.1	0.4	0.4
GVS-93	12	19	13	15	341	361	364	355	5.1	1.4	2.5	3.0
GVS-94	19	24	24	22	539	429	448	472	-0.4	1.2	1.8	0.9
GVS-100-01	22	20	22	21	853	613	961	809	2.0	1.0	1.7	1.5
GVS-100-02	293	173	160	208	1817	1529	1710	1685	0.6	1.0	3.4	1.7
GVS-107	66	75	85	75	571	634	570	592	NM	1.5	-0.9	0.3
GVS-110	21	16	16	18	455	598	537	530	2.0	2.2	2.5	2.2
GVS-111	19	19	20	19	711	733	709	718	0.7	3.2	3.5	2.5
GVS-114	13	14	15	14	364	428	451	414	2.7	2.9	2.9	2.9
GVS-118	19	11	12	14	581	301	272	385	0.6	1.5	0.1	0.7
GVS-121	32	32	33	33	929	840	1339	1036	3.4	0.9	-0.2	1.4
GVS-123	17	26	27	23	736	612	1045	798	2.5	-0.6	0.2	0.7
TR-419	14	14	12	13	602	417	613	544	-1.1	0.4	0.3	-0.1[1]
TR-503	12	19	19	16	335	327	309	323	0.8	0.5	0.9	0.7
TR-513	24	23	21	22	317	381	492	397	-0.9	0.5	0.0	-0.1[1]
TR-517	17	14	11	14	293	279	260	277	0.6	3.9	1.9	2.1
TR-531	17	15	9	14	132	122	138	131	-0.6	-0.2	0.6	-0.1[1]
TR-614	9	7	7	8	228	202	216	216	-0.1	0.9	0.0	0.3
TR-616	26	44	37	36	1044	956	828	943	0.5	1.9	0.9	1.1
TP-006-003	5	6	8	6	475	484	490	483	-0.5	0.6	-0.7	-0.2[1]
TP-006-004	9	9	9	9	406	400	388	398	-1.5	0.6	0.7	-0.1[1]
TP-006-005	8	11	6	8	715	704	658	692	-1.4	1.0	4.2	1.3

[1]ion concentration at steady-state was higher than control experiment

NM = not measured

Standard deviation of each average and standard deviation of the three replicates is provided in Appendix A.

Table 5. Previously reported K$_d$ values for cementitious materials under oxidizing and reducing conditions.

Element	Best Oxidizing Cement K$_d$ Young	Best Oxidizing Cement K$_d$ Middle	Best Oxidizing Cement K$_d$ Old	Best Reducing Cement K$_d$ Young	Best Reducing Cement K$_d$ Middle	Best Reducing Cement K$_d$ Old
Cs	2	20	10	2	20	10
Sr	15	15	5	15	15	5
I	8	15	4	5	9	4

SRNL-STI-2009-00473

4.1 CESIUM MEASURED IN CEMENTITIOUS MATERIALS

The Cs K_d values ranged from 6.3 to 370 mL/g and the mean was 44.5 ± 84 mL/g (Table 6) in this test and are compared with reported values of 2 and 20 for young and middle cement, respectively (Table 6) (Kaplan 2009). This experimentally derived range is extremely wide, wider than the mean; coefficient of variation is 189% (CV = standard deviation/mean x 100); Table 6). The wide range of K_d values obtained was in part the result of the range of recipes used to make the saltstone (varying simulant, premix ratios, water to premix, aluminate, temperature curing, sample age). This range of condition was selected to approximate conditions that may exist under field conditions, where mixing may be difficult to control. In closer statistical examination of the data, much of this variance can be attributed to two data, GVW-88 (K_d 370 mL/g) and GVS-100-02 ($K_d = 208$ mL/g); both these samples were heat treated to 60 ^{o}C (Table 3 and 4). This was further evaluated statistically by asking if these two data represent another population, i.e., if these two data points are outliers (see the 2-component normal fit to the Cs distribution data in Appendix A; Table 26). There was not sufficient data to demonstrate a separate population, but a trend appears. Furthermore, regression analysis between temperature (Table 3 and 4) and Cs K_d resulted in a significant correlation ($r = 0.59$; significant at $P \leq 0.05$). The regression was strongly driven by the two points and was not a continuous trend. When the Cs K_d values were categorized by temperature, again there appeared to be an indication of temperature dependence on Cs K_d values:

- all data $K_d = 45 \pm 84$ mL/g (n = 22);
- 60°C $K_d = 289 \pm 115$ mL/g (n = 2);
- <60°C $K_d = 20 \pm 15$ mL/g (n = 20);
- 22°C $K_d = 18 \pm 15$ mL/g (n = 15)

Additional related statistics are in Appendix A. It is anticipated that upon further research the influence of temperature effect on sorption will be better understood and the range of values will be greatly contracted. At present, the full range of temperature conditions at the saltstone facility are not fully known and the impact of curing temperature on cement-phase mineral formation and subsequent radionuclide sorption. This is discussed in more detail in Section 4.5.

In the literature, Cs K_d values in hardened HTS cement discs (Haute Teneure en Silice, a French sulphate resistant cement), pH 13.3 were close to 3 mL/g (Sarott et al. 1992). Wieland and Van Loon (2003) reviewed Cs K_d values of various cementitious materials and they had a very narrow range of 0.2 to 5 mL/g. Kaplan and Coates (2007) measured cesium K_d values in Ca(OH)$_2$-saturated and Ca-CaCO$_3$-saturated solutions in ground, 40-year old concrete, simulating 1st/2nd and 3rd Stages, respectively. Measured K_d values were 21, and 17.6 mL/g, respectively.

Table 6. Plots and descriptive statistics for Cs K_d values in saltstone

Distribution of the Mean(Cs-K_d)	Distribution of the Log_e(Mean(Cs-K_d))

Quantiles			Quantiles		
100.0%	maximum	369.667	100.0%	maximum	5.9126
99.5%		369.667	99.5%		5.9126
97.5%		369.667	97.5%		5.9126
90.0%		168.667	90.0%		5.03509
75.0%	quartile	25.5833	75.0%	quartile	3.23144
50.0%	median	17.1667	50.0%	median	2.84255
25.0%	quartile	13.5833	25.0%	quartile	2.60879
10.0%		7.86667	10.0%		2.0619
2.5%		6.33333	2.5%		1.84583
0.5%		6.33333	0.5%		1.84583
0.0%	minimum	6.33333	0.0%	minimum	1.84583

Moments		Moments	
Mean	44.545455	Mean	3.0780819
Std Dev	84.212351	Std Dev	0.9933274
Std Err Mean	17.954134	Std Err Mean	0.2117781
Upper 95% Mean	81.883119	Upper 95% Mean	3.5184986
Lower 95% Mean	7.2077898	Lower 95% Mean	2.6376652
N	22	N	22
Variance	7091.7201	Variance	0.9866994
Skewness	3.3630383	Skewness	1.6753091
Kurtosis	11.540562	Kurtosis	2.9279735
CV	189.04813	CV	32.270988
N Missing	0	N Missing	0

The data distribution in Table 6 also demonstrates that the Cs K_d are clearly not normally distributed, especially when one looks at the "Distribution of the Mean(Cs-K_d)" data on the left in Table 6. The **skewness** value is a measure of the asymmetry of the probability distribution of a real-valued random variable. The positive skewness value means it tails to the right as shown in Table 6. The relatively large value (>3.0) of 3.36, suggest that the right tail is much longer than the left tail and that a normal distribution is not appropriate. Like skewness, kurtosis, is used to describe the probability distribution. **Kurtosis** is a measure of the "peakedness" of the

probability distribution. In Table 6, the kurtosis is relatively large value, suggesting a spreading of the distribution, as oppose to forming a sharp peak. Again, there are no other reported distributions of cementitious K_d values in the literature to compare these statistics.

4.1.1 Cesium K_d Model Comparisons of Distribution Fits:

Goodness of fit analysis of the 12 distribution models (discussed in Section 3.2.4) indicated that the (from best fit to worse fit) Frechet, Generalized Gamma, Loglogistic, and Lognormal distribution models had the best fit. Lower the goodness of fit value, the better the fit. Not surprising the normal distribution was not representative of the dataset (Table 6). The Frechet and Loglogistic distributions are presented in Figure 1. (The Generalized Gamma model was not considered when more simple models are available; it has a third fitting parameters, when the others generally only require two fitting parameters.) Frechet model is best on two of three global metrics. Extended Generalized Gamma does best on likelihood.

Table 7. Goodness-of-fit of distribution models for Cs K_d values in saltstone.

Distribution	AICc[a]	-2Loglikelihood	BIC
Frechet	192.32093	187.68936	193.87144
Generalized Gamma	194.02134	186.68801	195.96113
Loglogistic	197.89614	193.26456	199.44664
Lognormal	201.18246	196.55088	202.73297
Log Generalized Gamma	212.33922	205.00589	214.27902
Weibull	213.01320	208.38162	214.56370
Exponential	213.24645	211.04645	214.13749
LEV	233.58784	228.95627	235.13835
Logistic	247.30243	242.67085	248.85293
Normal	261.10846	256.47689	262.65897
SEV	279.85554	275.22396	281.40604

[a] AIC: Akaike information criterion; BIC: Schwartz's Bayesian information criterion; -2 log likelihood: -2 times the natural log of the likelihood evaluated with the best-fit estimates of the parameters

Frechet: quantile on left and nonparametric on right
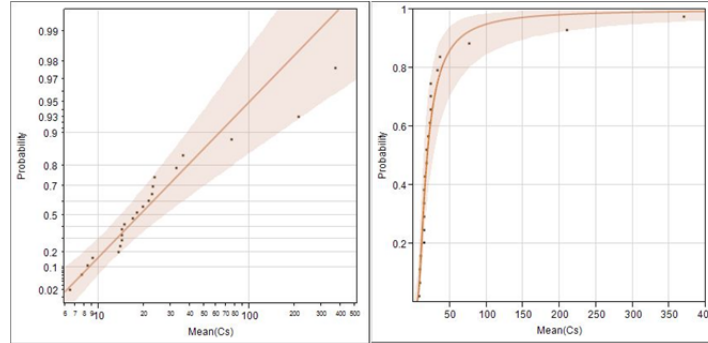
Loglogistic: quantile on left and nonparametric on right
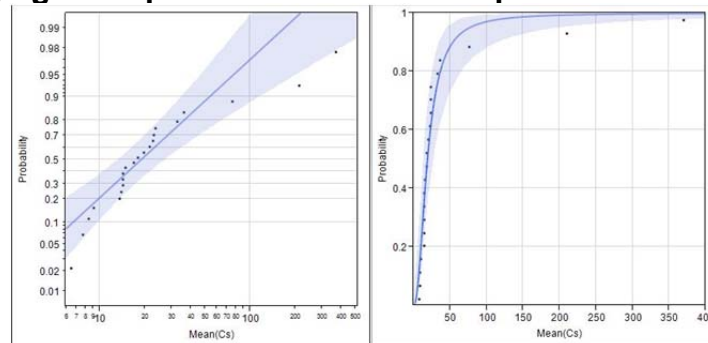
Lognormal: quantile on left and nonparametric on right
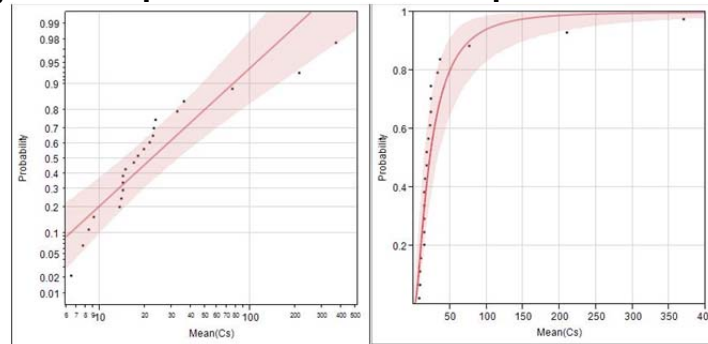
Figure 1. (TOP) The Frechet distribution of the Cs K_d Saltstone data set. Plot on left (quantile) is a linear version of plot on right (nonparametric). Shaded region provides 95% confidence region. Note no points outside shaded zone. Frechet distribution fits the low- and mid K_d values especially well. (MIDDLE) The Loglogistic distribution of the Cs K_d saltstone data set quantile (left) and nonparametric (right). Note that there are three or four data points outside the shaded region and the low K_d fit is poor even though the general goodness-of-fit is very acceptable. (BOTTOM) Lognormal distribution of Cs K_d saltstone data set quantile (left and nonparametric (right) Of the three models, this one is the poorest.
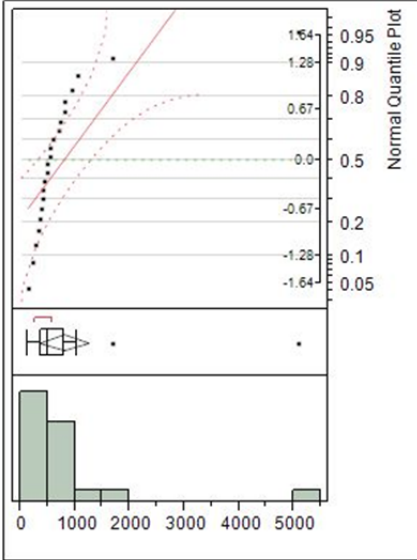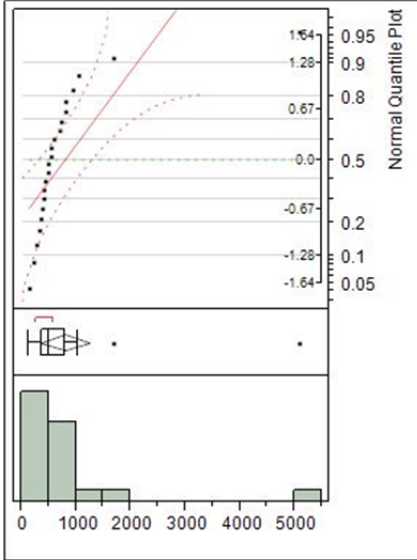
4.2 STRONTIUM K_d VALUES MEASURED IN CEMENTITIOUS MATERIALS

The Sr K_d values ranged from 131 to 5080 and had a mean of 785 ± 1016 (Table 8). Again, the distribution is extremely large, greater than the mean, with a coefficient of variation (standard deviation/mean x 100) of 129%. Like the distribution of the Cs K_d values, this wide variation appears to stem primarily from one or at most three samples. This is easiest seem in the histogram of the data distribution in Table 8. Looking at the individual data points in Table 4 the three largest K_d values were from sample GVS-88 (K_d = 5080 mL/g), GVS-100-02 (K_d =1685 mL/g) and GVS-121 (1036 mL/g); the first two had some form of a 60° C heat treatment (Table 3). The values reported here are more in line with those reported in desorption experiments with actual saltstone sample recovered from the Saltstone Facility (Almond and Kaplan 2011). Those samples, in which the Sr was desorbed under oxidizing and reducing conditions, resulted in apparent K_d values of 737 and 5728 mL/g. These higher K_d values were attributed to the potential formation of Sr-sulfate phases and it was supported by the high apparent K_d under oxidizing than reducing conditions.

The currently reported K_d value for strontium in young and middle aged cementitious environments is identical, 15 mL/g (Table 5; Kaplan 2010).. Strontium typically has a moderately low K_d in cementitious environments; however, when sulfate concentrations are high, $SrSO_4$ precipitates, as was likely the case here. $SrSO_4$ has a solubility of 3.2E-07 M (strontium sulfite solubility product is even lower, $SrSO_3$ K_{sp} = 4E-08 M). Large Sr sorption was also noted under reducing conditions.

Jakubick et al. (1987) reported Sr K_d values of 0.8 to 1.6 mL/g for high density and normal density concretes, and 1.3 to 3 mL/g for the same concretes, but in lower ionic strength solutions. Ewart et al. (1986) reported K_d values between 1 and 4 mL/g. Kato and Yanase (1993) reported a Sr K_d value of 56 mL/g for an experiment involving 24 h contact time, dried cement powder, pH 11 cement equilibrated water. Previously, we elected to disregard this value because it is an order-of-magnitude greater than those reported by other researchers and the nature of the solid phase was not clearly described by the author. In 1st Stage K_d values were decreased because high ionic strength likely results in competitive exchange (desorption). Kaplan and Coates (2007) measured Sr K_d values in Ca(OH)-saturated and $CaCO_3$-saturated solutions in ground, 40-yr old concrete, simulating 1st/2nd and 3rd Stages, respectively. The measured K_d values were 28.1 and 39.1 mL/g, respectively.

Table 8. Plots and descriptive statistics for Sr K_d values in saltstone

Distribution of the Mean(Sr-K_d)	Distribution of the Log(Mean(Sr-K_d)

Quantiles			Quantiles		
100.0%	maximum	5,080	100.0%	maximum	8.53307
99.5%		5,080	99.5%		8.53307
97.5%		5,080	97.5%		8.53307
90.0%		1490.53	90.0%		7.28374
75.0%	quartile	800.5	75.0%	quartile	6.68522
50.0%	median	506.5	50.0%	median	6.22645
25.0%	quartile	377.333	25.0%	quartile	5.93255
10.0%		233.933	10.0%		5.4481
2.5%		130.667	2.5%		4.87265
0.5%		130.667	0.5%		4.87265
0.0%	minimum	130.667	0.0%	minimum	4.87265

Moments		Moments	
Mean	785.33333	Mean	6.3186987
Std Dev	1016.8829	Std Dev	0.744799
Std Err Mean	216.80017	Std Err Mean	0.1587917
Upper 95% Mean	1,236.194	Upper 95% Mean	6.6489241
Lower 95% Mean	334.4727	Lower 95% Mean	5.9884733
N	22	N	22
Variance	1034050.9	Variance	0.5547255
Skewness	3.9282015	Skewness	1.0326982
Kurtosis	16.76389	Kurtosis	2.9936167
CV	129.48424	CV	11.787221
N Missing	0	N Missing	0

4.2.1 Strontium K_d Model Comparisons of Distribution Fits

Goodness of fit analysis of the 12 distribution models (Section 3.2.4) indicated that the (from best fit to worse fit) Loglogistic, Frechet, Lognormal, and Generalized Gamma distribution models had the best fit (Table 9). Lower the goodness of fit value, the better the fit. Again, not surprising the normal distribution was not representative of the dataset (Table 8). The Frechet

and Loglogistic distributions are presented in Figure 2. The Generalized Gamma model was not considered when more simple models were available; it has a third fitting parameters, whereas the others generally only require two fitting parameters.

Table 9. Goodness-of-fit of distribution models for Sr K$_d$ values in saltstone.

Distribution	AICc [a]	-2Loglikelihood	BIC
Loglogistic	328.72148	324.08991	330.27199
Frechet	329.92418	325.29260	331.47469
Lognormal	331.09998	326.46840	332.65048
Generalized Gamma	331.66867	324.33534	333.60846
Log Generalized Gamma	337.12898	329.79564	339.06877
Exponential	339.50876	337.30876	340.39981
Weibull	341.44548	336.81390	342.99598
LEV	343.48815	338.85657	345.03865
Logistic	354.48205	349.85047	356.03255
Normal	370.71931	366.08773	372.26982
SEV	391.75553	387.12395	393.30604

[a] AIC: Akaike information criterion; BIC: Schwartz's Bayesian information criterion; -2 log likelihood: -2 times the natural log of the likelihood evaluated with the best-fit estimates of the parameters
Frechet is best on 2 of 3 global metrics. Extended Generalized Gamma does best on likelihood.
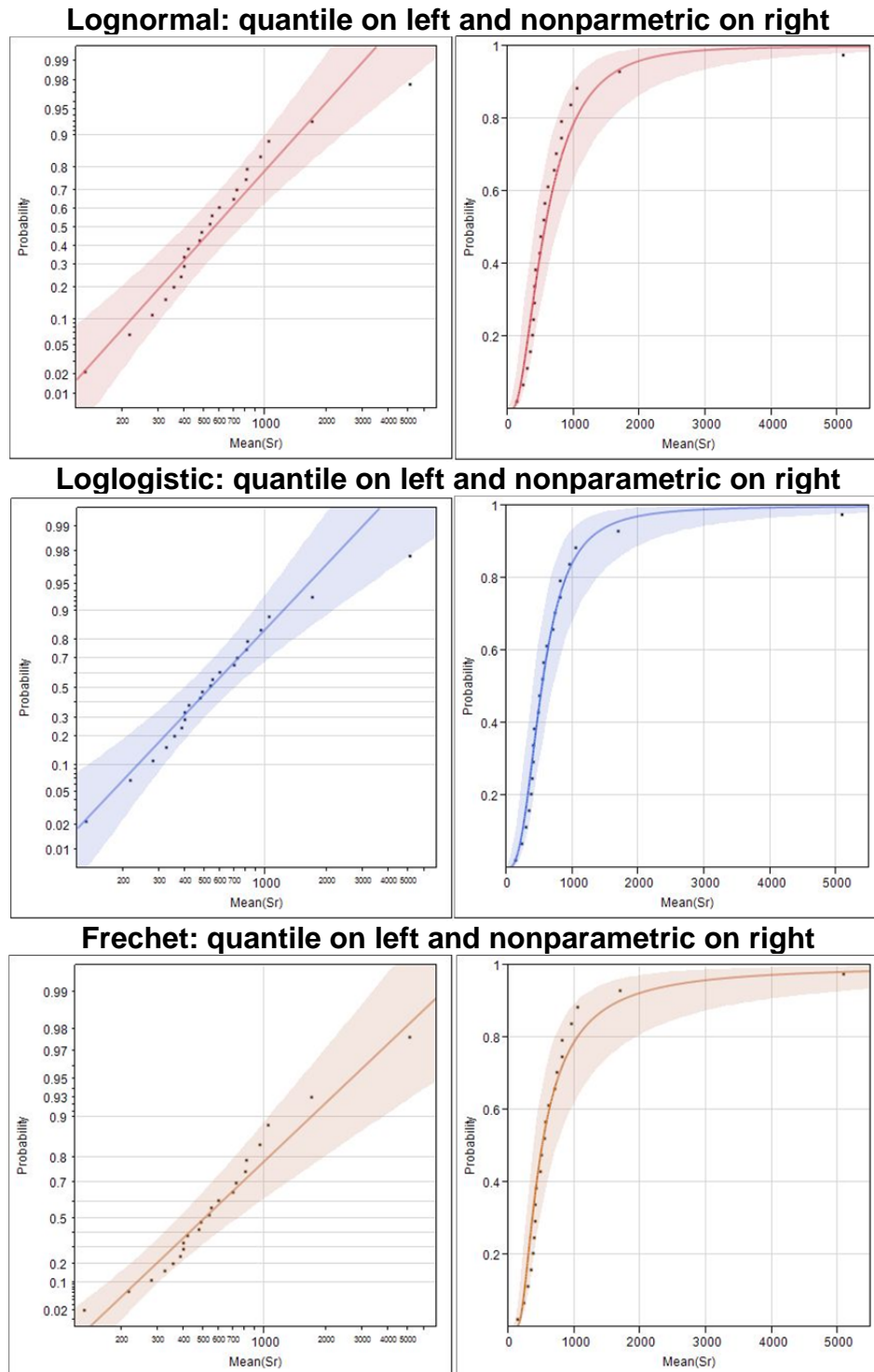
Figure 2. Lognormal, loglogistic and Frechet quantile and nonparametric plots of the Sr K_d Saltstone data. Shaded region provides 95% confidence region. Compared to the Frechet, the loglogistic distribution seems to be a bit better than the Frechet for low K_d values, and near the "elbow" of the graph.

4.3 IODINE MEASURED IN CEMENTITIOUS MATERIALS

The K_d values ranged from -0.2 to 3.0 (Table 4). But it was decided that the negative K_d values were not physically meaningful for this system and could not be handled with some of the distribution models. For statistical purposes the negative K_d values were reassigned to zero values. Our lab has reported anion exclusion, or negative K_d values to TcO_4^- to highly negatively charge sediments (not SRS sediments) (Kaplan and Serne 1998), but this system does not at present support assigning negative K_d values. The negative K_d values in Table 4 suggest that the negative K_d values stems more from analytical uncertainty than from anion exclusion (see samples TR-419,TR-513, TR-531, and TP-006-003). This is acceptable analytical error at these low K_d values.

The mean iodine K_d value is 1.0 ± 0.97 mL/g (Table 10). The somewhat narrower standard deviation compared to the Cs and Sr K_d value measured values is likely real due to the generally low K_d values as well as to the fact that the K_d range was artificially truncated at 0 mL/g. The skewness and kurtosis is also low, suggesting that the data is evenly distributed and has a peak (is not flat; these terms are discussed in section 3.2.4.)

Table 10. Plot and descriptive statics for iodine K_d values in saltstone.

Distribution of the Mean(Iodine-K_d)

Quantiles		
100.0%	maximum	3
99.5%		3
97.5%		3
90.0%		2.72333
75.0%	quartile	1.78333
50.0%	median	0.8
25.0%	quartile	0.2
10.0%		0
2.5%		0
0.5%		0
0.0%	minimum	0

Moments	
Mean	1.0727273
Std Dev	0.972513
Std Err Mean	0.2073405
Upper 95% Mean	1.5039154
Lower 95% Mean	0.6415391
N	22
Variance	0.9457816
Skewness	0.6148053
Kurtosis	-0.777313
CV	90.657996
N Missing	0
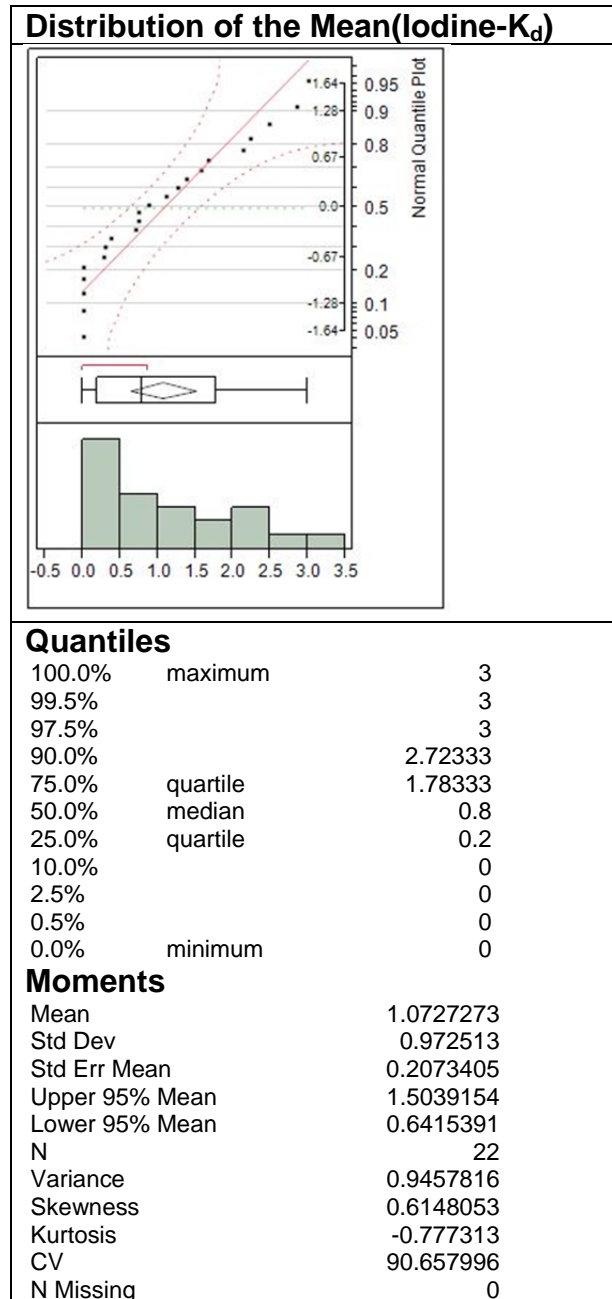
4.3.1 Iodine K_d Model Comparisons of Distribution Fits

One difference with the iodine data was that there were negative values and as mentioned above, it is believed that there is not negative adsorption (anion exclusion) occurring (Table 4). Negative values in the distribution would require special consideration for distributions. Rather than delete these values from the data set, they were set to zero. The logic was, it is better to

weigh the data set low, then to delete the data and not acknowledge their presence in the dataset. Then distribution model fit analyses were conducted using zero-inflated distributions. This essentially means that there are more zero K_d's (realistically small K_d's) than one might expect. This surplus of small values does not affect the fit of the distribution to the positive K_d values and in essence, the distribution treats the fit of the data as if there is two groups of data, the data equal to zero, and the non-zero data. The origin of zero-inflated distributions comes from reliability studies where a certain segment of the population cannot respond or has failed prior to being put on test. In the current case we have selected a surplus of zero K_d samples.

Four zero-inflated distributions were tried: Weibull, lognormal, loglogisitc, and Frechet (Table 11). Here are the goodness-of-fit statistics. Smallest values indicate the best fit to the data. (AIC: Akaike information criterion; BIC: Schwartz's Bayesian information criterion; -2 log likelihood: -2 times the natural log of the likelihood evaluated with the best-fit estimates of the parameters). The zero-inflated Weibull, Lognormal and Loglogistic distribution had reasonably general fits to the data. Only the zero-inflated Weibull distribution seems to fit the data well between the K_d values of 1 and 2 mL/g. The Weibull is the best for all three global criterions. Note that the fitted line in all cases does not attempt to intercept the data at 0 mL/g; instead the predicted line runs parallel to the x-axis from the last data point (K_d ~0.3/P~0.22). This low data fit to the data is unique to the zero-inflated distribution models.

Table 11. Goodness-of-fit of distribution models for iodine K_d values in saltstone.

Distribution	AICc [a]	-2Loglikelihood	BIC
Zero Inflated Weibull	50.172673	42.839339	52.112467
Zero Inflated Lognormal	51.760036	44.426703	53.699830
Zero Inflated Loglogistic	52.772682	45.439349	54.712476
Zero Inflated Frechet	55.530240	48.196906	57.470034

[a] AIC: Akaike information criterion; BIC: Schwartz's Bayesian information criterion; -2 log likelihood: -2 times the natural log of the likelihood evaluated with the best-fit estimates of the parameters
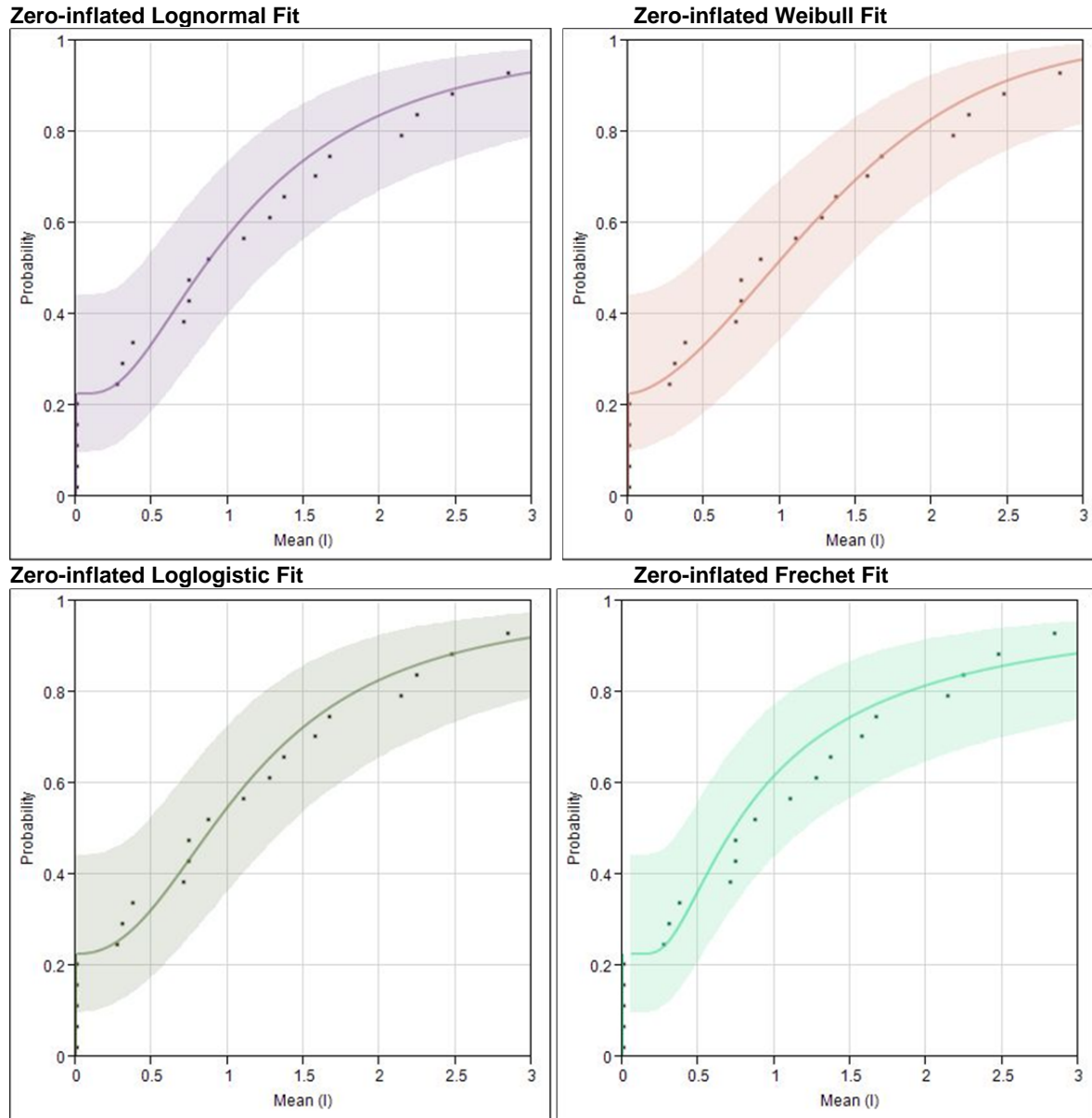
Figure 3. Zero-inflated distribution models to the iodine saltstone K_d values: Lognormal, Weibull, Loglogistic, and Frechet. The "Zero-inflated" indicates that the negative K_d values were assigned zero values and treated uniquely in the distribution model.

4.4 EUROPIUM MEASURED IN CEMENTITIOUS MATERIALS

Precipitation of Eu precluded the ability to calculate K_d values. Eu concentrations were below detection limits for all samples in the no-solids controls and in the samples containing cementitious solids. Therefore the measured decreases in aqueous radionuclides were due to causes other than the sorption of the radionuclides by the added solid phases.

4.5 EFFECT OF CEMENT CURE TEMPERATURE ON DISTRIBUTION COEFFICIENTS IN CEMENTITIOUS MATERIALS

Analysis of samples that were heated to 60 °C during curing for a short period of time (days) immediately after mixing demonstrated a marked improvement in K_d for Cs and Sr over samples cured between room temperature and ~55 °C (Table 4). Cure temperatures at or above ~60 °C change the physical properties of saltstone and this phenomenon may contribute to mechanisms that encourage sorption or precipitation of elements, such as Cs and Sr over room-temperature cured samples.

Metastable hydrates exist in cementitious materials at 25 °C. As temperature is increased, substantial changes in cement chemistry can be observed in blended cement phases. Glasser et al. (1991) performed a temperature effects study with cements containing BFS and OPC or FA. Results indicate that significant changes in $Ca(OH)_2$ were observed for samples that were cured at 56 and 72 °C versus room temperature. Regardless of cure temperature, little change in $Ca(OH)_2$ was observed between 3 months and 1 year, indicating that reactions between BFS and $Ca(OH)_2$ to produce C-S-H continued at a slow rate or had stopped.

Glasser et al. reported XRD patterns of cementitious material containing a mixture of BFS and OPC at room temperature indicated ettringite, monosulfate, and $Ca(OH)_2$ as the predominant (and expected) hydration products. However, samples cured to at 56 or 72 °C, aside from having reduced $Ca(OH)_2$ levels, were absent of (or had significantly reduced) monosulphate, yet had an ingrowth of hydrogarnet.

Changes in hydration products resulting from elevated cure temperatures may affect mechanisms that control retention of ions in saltstone materials. Further investigation of the phases formed in saltstone samples heated at or above 60 °C while curing may help explain and validate the variability of K_d values observed for this select group of samples.

Previous experiments with SRNL-prepared laboratory samples have shown that increase in cure temperature can effect physical properties such as heat of hydration, dynamic Young's modulus, porosity, compressive strength, and set time (Harbour 2009).

4.6 PLUTONIUM DISTRIBUTION COEFFICIENTS MEASURED IN SOILS

The sediment Pu K_d data is included in this study because it is a potential risk driver for the SRS PAs, and there are presently no direct studies of Pu variability in SRS soils. Instead the distribution of Pu sediment K_d values was assumed to be similar to other cations, as presented by

Kaplan (2010). The sediments used in this portion of the study were selected by a number of criteria identified in the Materials and Methods section, including the origin of soil, Pu oxidation state, and contact time with sediment (Table 12). They were further broken down into three broad categories to simulate three general types of plume:

- a far-field plume: pH 4.6 to 7.0,
- a high pH plume: pH >7.0, and
- a plume moving through a pH 4.6 to pH 10.47 system.

Much of the Pu sorption data that is reported as K_d values, especially the high pH Pu(IV) sorption data, indicates that Pu in the system has precipitated, as the reports demonstrated with the formation of Pu(IV) phases. Also, cement leachate is expected to be greater than pH 10.47, the largest pH value for which sorption experimental data was found. Higher pH data is necessary to confirm how soils will behave between 10.5 and pH 12. The properties of the sediments described in Table 12 are presented in Table 13.

Table 12. Pu K_d values selected from the literature used to develop the Pu K_d sediment distribution (sorted by pH).

Soil	pH	K_d (mL/g)	Contact time (day)	source	Spike Pu Oxidation State
surface clay	4.63	3000	1	WSRC-TR-2003-00035; page 48	4
surface clay	4.67	13000	33	WSRC-TR-2003-00035; page 48	5
Subsurface Sand	4.69	110	33	WSRC-TR-2003-00035; page 46	5
Subsurface Sand	4.72	130	33	WSRC-TR-2003-00035; page 46	5
surface sand	4.78	1200	33	WSRC-TR-2003-00035; page 50	5
Subsurface Clay	4.81	2100	1	WSRC-TR-2003-00035; page 47	4
surface sand	4.82	510	6	WSRC-TR-2003-00035; page 49	5
Subsurface Sand	4.87	100	33	WSRC-TR-2003-00035; page 46	5
Subsurface Clay	4.95	9300	33	WSRC-TR-2003-00035; page 47	5
Subsurface Sand	5.10	600	33	WSRC-TR-2003-00035; page 46	5
Subsurface Sand	5.21	4800	33	WSRC-TR-2003-00035; page 46	5
Subsurface Sand	5.23	3700	33	WSRC-TR-2003-00035; page 46	5
surface sand	5.26	2900	6	WSRC-TR-2003-00035; page 49	5
Subsurface Clay	5.32	10000	33	WSRC-TR-2003-00035; page 47	5
Subsurface Sand	5.41	4900	33	WSRC-TR-2003-00035; page 46	5
Subsurface Sand	5.62	3100	33	WSRC-TR-2003-00035; page 46	5
surface clay	5.67	13000	33	WSRC-TR-2003-00035; page 48	5
Subsurface Clay	5.68	4700	33	WSRC-TR-2003-00035; page 47	5
Subsurface Clay	5.82	6600	1	WSRC-TR-2003-00035; page 47	4
surface sand	5.83	1400	6	WSRC-TR-2003-00035; page 49	5
Subsurface Sand	5.85	390	1	WSRC-TR-2003-00035; page 46	4
Subsurface Clay	5.98	9000	1	WSRC-TR-2003-00035; page 47	4
surface clay	6.02	4600	1	WSRC-TR-2003-00035; page 48	4
surface clay	6.05	13000	33	WSRC-TR-2003-00035; page 48	5
surface clay	6.09	1000	1	WSRC-TR-2003-00035; page 48	4
Subsurface Sand	6.10	2800	1	WSRC-TR-2003-00035; page 46	4
surface sand	6.13	1800	6	WSRC-TR-2003-00035; page 49	5
surface sand	6.34	1700	6	WSRC-TR-2003-00035; page 49	5
surface clay	6.55	8200	33	WSRC-TR-2003-00035; page 48	5
surface sand	6.56	400	6	WSRC-TR-2003-00035; page 49	5
Subsurface Sand	6.61	2500	1	WSRC-TR-2003-00035; page 46	4
surface sand	6.61	8300	33	WSRC-TR-2003-00035; page 50	5
Subsurface Clay	6.68	18000	1	WSRC-TR-2003-00035; page 47	4
surface sand	6.73	130	1	WSRC-TR-2003-00035; page 49	4
surface clay	6.81	33000	33	WSRC-TR-2003-00035; page 48	5
surface clay	6.83	3700	1	WSRC-TR-2003-00035; page 48	4
surface sand	6.89	8300	33	WSRC-TR-2003-00035; page 50	5
surface sand	6.98	270	6	WSRC-TR-2003-00035; page 49	5
surface sand	7.00	5700	33	WSRC-TR-2003-00035; page 50	5
Surface Sand	7.00	20000	33	WSRC-TR-2003-00035; page 50	5
Surface Clay	7.11	3500	1	WSRC-TR-2003-00035; page 48	4
Subsurface Clay	7.16	1600	33	WSRC-TR-2003-00035; page 47	5
Surface Clay	7.22	8200	33	WSRC-TR-2003-00035; page 48	5

Soil	pH	K_d (mL/g)	Contact time (day)	source	Spike Pu Oxidation State
Subsurface Clay	7.32	3700	33	WSRC-TR-2003-00035; page 47	5
Surface Clay	7.36	33000	33	WSRC-TR-2003-00035; page 48	5
Surface Sand	7.36	20000	33	WSRC-TR-2003-00035; page 50	5
Surface Sand	7.36	20000	33	WSRC-TR-2003-00035; page 50	5
Surface Clay	7.49	33000	33	WSRC-TR-2003-00035; page 48	5
Surface Clay	7.53	13000	33	WSRC-TR-2003-00035; page 48	5
Surface Sand	7.58	20000	33	WSRC-TR-2003-00035; page 50	5
Subsurface Clay	7.69	1300	33	WSRC-TR-2003-00035; page 47	5
Subsurface Sand	7.70	2800	1	WSRC-TR-2003-00035; page 46	4
Subsurface Clay	7.74	600	33	WSRC-TR-2003-00035; page 47	5
Subsurface Clay	7.79	42000	1	WSRC-TR-2003-00035; page 47	4
Surface Sand	7.86	20000	33	WSRC-TR-2003-00035; page 50	5
Subsurface Clay	7.91	50000	1	WSRC-TR-2003-00035; page 47	4
Surface Sand	8.26	210	6	WSRC-TR-2003-00035; page 49	5
Subsurface Sand	8.42	20000	1	WSRC-TR-2003-00035; page 46	4
Surface Clay	8.49	1300	1	WSRC-TR-2003-00035; page 48	4
Subsurface Clay	8.89	540	33	WSRC-TR-2003-00035; page 47	5
Surface Clay	9.15	3300	33	WSRC-TR-2003-00035; page 48	5
Subsurface Sand	9.28	9300	1	WSRC-TR-2003-00035; page 46	4
Surface Clay	9.95	800	1	WSRC-TR-2003-00035; page 48	4
Surface Sand	10.47	290	1	WSRC-TR-2003-00035; page 49	4

[a] An SRS Pu K_d data set that was purposely not included here was that of Prout (1958). The reason was because the SRS sediments were not characterized, experimental protocol was not specified in sufficient detail, and contact time was only one day,

Table 13. Characterization of sediments used in Pu K_d measurements discussed in Table 12.

Soil	Subsurface Clay	Subsurface Sand	Surface Clay	Surface Sand
% sand (>53 μm)	57.9	97	68	92
% silt (53 – 2 μm)	40.6	2.9	24	7
% clay (<2 μm)	1.6	0.2	8	1
Textural classification	Silty clay	Sand		
pH[a]	4.55	5.1	5.8	4.7
% OM [b]	1.21	0.35	3.2	0.8
CEC (cmol/kg) [e]	1.09 ± 0.31	-0.35 ± 0.22		
AEC (cmol/kg) [e]	1.58 ± 0.61	0.06 ±0.19		
BET surface area (m^2/g)	15.31	1.27	9.2	1.4
Single point surface area (m^2/g)	15.07	1.24		
CDB extractable Fe (mg/g) [c]	15.26	7.06		
Al (ppm)	63.59	16.64		
Na (ppm)	42.91	34.69		
Mg (ppm)	144.05	98.76		
Ca (ppm)	64.41	24.62		
K (ppm)	182.87	92.97		
Mineralogy (based on XRD)	Kao > goeth > Hem (no qtz or 14 A)	Kao > goeth >musco/14A (no qtz)	Kao > chlorite/verm . qtz > goeth > gibb > rutile	Chlorite/vermiculite > quartz > kaolinite >illite

[a] pH procedure from Chemical Analysis of Ecological Materials, Stewart E. Allen, pgs. 16-17.
[b] OM procedure from Chemical Analysis of Ecological Materials, Stewart E. Allen, pgs. 15-16.
[c] CDB procedure from Methods of Soil Analysis Part 3-Chemical Methods, D.L. Sparks pgs 1228-1220.
[d] Ion extraction procedure from Methods of Soil Analysis Part 3-Chemical Methods, D.L. Sparks pgs 1218-1220; 0.2 M NH$_4$Cl.
[e] CEC/AEC procedure from Methods of Soil Analysis Part 3-Chemical Methods, D.L. Sparks pgs 1218-1220; Unbuffered Salt Extraction Method.

4.6.1 Entire Pu K_d Data Set: All pH Values

The Pu K_d values ranged from 107 to 50,000 and the mean was $8559 \pm 11,241$ mL/g (Table 14). This is not an unexpected standard deviation considering the wide range of conditions that the K_d values were measured under and the wide variety of Pu species that exist in SRS sediments between pH 4.6 and 11 (unlike the almost uniform speciation of Cs^+ in groundwater). The coefficient of variance (CV) or percent standard deviation is over 100% and there is positive skewness, so the data is far from normal or symmetrical.

This large range of Pu K_d values is not uncommon under natural environmental conditions due to the wide range of parameters that influence Pu sorption to sediments (e.g., oxidation state, pH, natural organic matter, mineralogy, microbial populations, Eh, Fe-oxide coatings). There are three estimates of Pu K_d values ranges in nature, albeit, not under SRS site specific conditions:

- Thibault et al. (1990) reported a range in sandy soils of 27 to 36,000 mL/g with a geometric mean of 550 mL/g based on a literature review
- Baes and Sharp (1983) reported a range in agricultural soils of 11 to 300,000 mL/g in agricultural soils with a mean of geometric mean of 1800 mL/g, based on a literature review and thermodynamic calculations.
- Coughtrey et al. (1985) reported a range of Pu K_d in all sediments 18 to 10,000 mL/g with a best estimate of 5000 mL/g.

The range of 100 to 50,000 and a median of 3,700 is consistent with those previously reported. The smaller range can be attributed to the fact that only sediments from one location, the SRS, were included in this distribution.

Table 14. Quantiles and descriptive statistics of the full data set of Pu K_d values.

Quantiles and Descriptive Statistics for K_d		
100.0%	maximum	50,000
99.5%		50,000
97.5%		44,800
90.0%		20,000
75.0%	quartile	13,000
50.0%	median	3,700
25.0%	quartile	1,250
10.0%		282
2.5%		106.5
0.5%		100
0.0%	minimum	100
Descriptive Statistics		
Mean		8559.6923
Std Dev		10823.635
Std Err Mean		1342.5067
Upper 95% Mean		11241.658
Lower 95% Mean		5877.7268
N		65
Variance		117151081
Skewness		1.9212208
Kurtosis		3.7264401
CV		126.44888
N Missing		0

Table 15 provides the goodness-of-fit for the full data set of the Pu K_d values. It is a rank ordering from best to worst. Three global metrics for a good fit were used. The Weibull model had the best overall fit on two of three measures, since it has lower values for those metrics.

Table 15. Goodness-of-fit of distribution models for full data set of K_d values in soil.

Distribution	AICc	-2Loglikelihood	BIC
Weibull	1,301	1,296.8	1,305
Generalized Gamma	1,303	1,296.6	1,309
Lognormal	1,305	1,300.6	1,309
Loglogistic	1,308	1,303.7	1,312
Exponential	1,309	1,307.1	1,311
Log Generalized Gamma	1,314	1,307.8	1,320
Frechet	1,320	1,315.5	1,324
LEV	1,358	1,353.7	1,362
Logistic	1,384	1,380.3	1,389
Normal	1,395	1,391.1	1,399
SEV	1,436	1,432.1	1,440

[a] AIC: Akaike information criterion; BIC: Schwartz's Bayesian information criterion; -2 log likelihood: -2 times the natural log of the likelihood evaluated with the best-fit estimates of the parameters

A good fit is shown by the data points coming close to the straight line on the left of Figure 4.

Statistics give you a "global" view of what is a good fit. These plots show where the fit may be weak. Then it is up to the scientist together with the statisticians to decide whether it is a good fit. For example, the performance assessment may be more sensitive to low K_d values than high K_d values, and for this reason, we may select a model that is more accurate at fitting low K_d values than at fitting global K_d values identified by global goodness-of-fit parameters. Weibull appears to be the better fit, with possibly the exception of the lowest K_d value. As will be shown below, the Weibull distribution will also be a reasonable fit for the pH 4.6 to 7 data set and for the pH >7.0 data set.

Lognormal Fits: Left (quantile plot: log scale on x-axis)) and Right (nonparmetric plot)
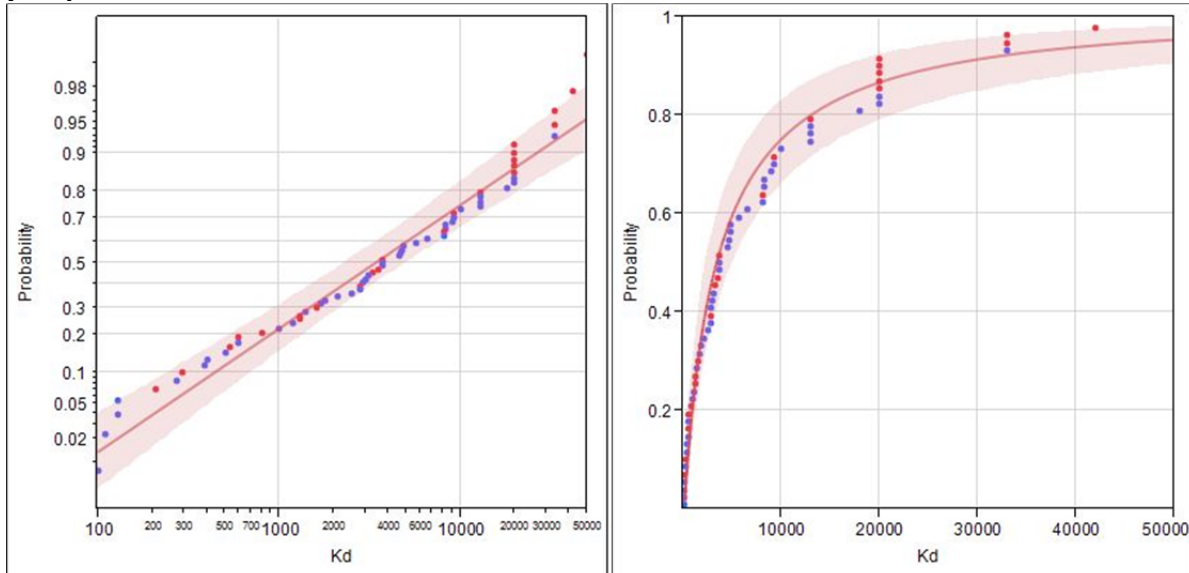
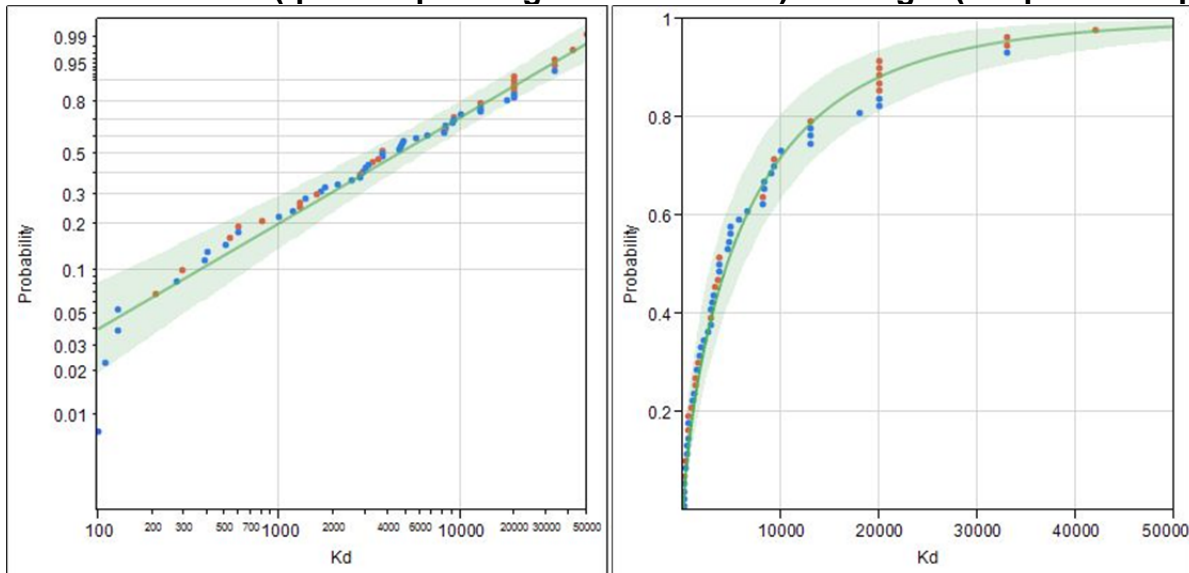**Weibull Fits: Left (quantile plot: log scale on x-axis) and Right (nonparmetric plot)**

Figure 4. Lognormal and Weibull distribution fits to the entire data set of sediment Pu K_d values. The red dots indicate pH>7.0 and blue dots indicate pH≤7. Shaded area is the 95% confidence region.

4.6.2 pH >7.0 Pu K_d Data Set

The range of Pu K_d values is 210 to 50,000 and the mean is $12,851 \pm 14,525$ (Table 16). Again, the skewness and kurtosis suggests that the shape of the distribution is not symmetrical, although in this case the peak of the curve, it is not nearly as flat as some of the previous distributions (kurtosis). The coefficient of variance is quite high even though the pH range was greatly limited, suggesting that pH is not the only controlling factor of Pu K_d values.

Table 16. Quantiles and descriptive statistics of the pH >7.0 Pu K_d data set.

Quantiles and Descriptive Statistics for K_d		
100.0%	maximum	50,000
99.5%		50,000
97.5%		50,000
90.0%		37,500
75.0%	quartile	20,000
50.0%	median	5,950
25.0%	quartile	1,300
10.0%		415
2.5%		210
0.5%		210
0.0%	minimum	210
Descriptive Statistics		
Mean		12851.667
Std Dev		14525.527
Std Err Mean		2965.0109
Upper 95% Mean		18985.259
Lower 95% Mean		6718.0744
N		24
Variance		210990945
Skewness		1.1859828
Kurtosis		0.5875395
CV		113.02446
N Missing		0

Table 17 provides a goodness-of-fit for the pH>7.0 Pu K_d data set: lower the value, the better the distribution model fit to the data. The table provides a listing from best to worst. Three global metrics for good fit were used. The Weibull model had the best overall fit on all three measures.

Table 17. Goodness-of-fit of distribution models for the pH >7.0 Pu K_d data set.

Distribution	AICc	-2Loglikelihood	BIC
Weibull	502.92655	498.35512	504.71123
Exponential	504.32080	502.13898	505.31704
Lognormal	504.36121	499.78978	506.14589
Generalized Gamma	504.70366	497.50366	507.03782
Threshold Lognormal	505.99122	498.79122	508.32538
Loglogistic	506.50000	501.92857	508.28468
Frechet	508.29970	503.72828	510.08438
Log Generalized Gamma	509.40925	502.20925	511.74342
LEV	523.47072	518.89929	525.25540
Logistic	531.49327	526.92184	533.27794
Normal	531.67487	527.10344	533.45955

[a] AIC: Akaike information criterion; BIC: Schwartz's Bayesian information criterion; -2 log likelihood: -2 times the natural log of the likelihood evaluated with the best-fit estimates of the parameters
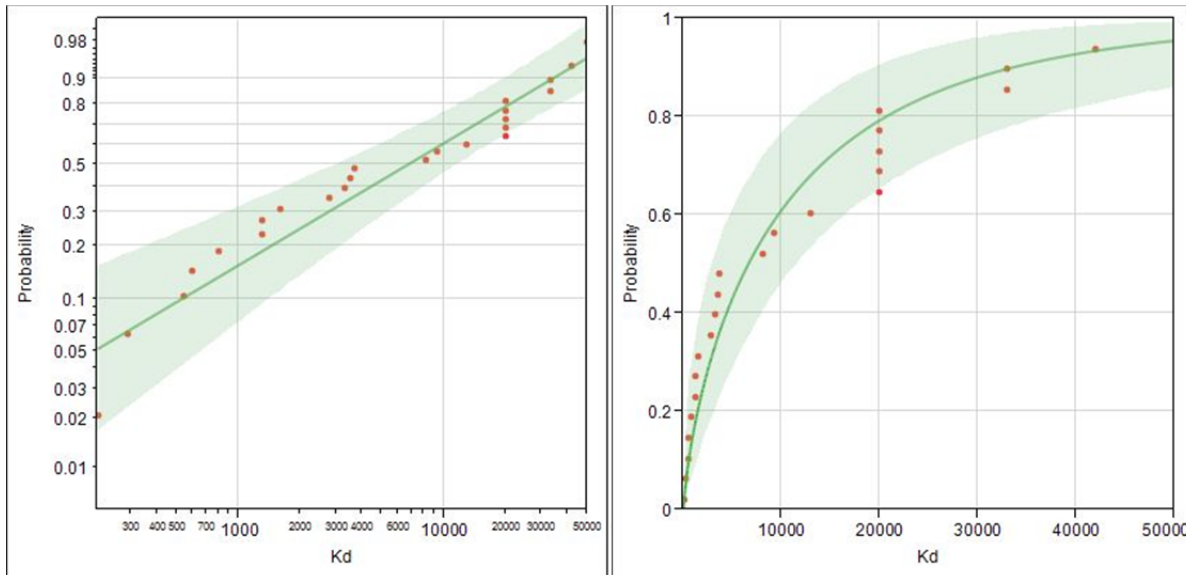

Figure 5. Weibull fits to the quantile plot (left) and nonparametric plot (right).

4.6.3 Pu K$_d$ Data Set for pH ≤7.0

The sediment Pu K$_d$ data ranged from 100 to 33,000 mL/g when the pH was restricted to 4.6 to 7.0 or less, simulating far-field conditions, the conditions far from the chemical influence from the source term (Table 18). The mean Pu K$_d$ was 6047 ± 6971 mL/g (Table 18). Again, the standard deviation is extremely large, as was the case with the entire data set indicating that limiting the pH does not reduce variance. The kurtosis is especially high, indicating the data is spread out.

Table 18. Quantiles and descriptive statistics of the pH ≤7.0 Pu K$_d$ data set.

Quantiles and Descriptive Statistics for K$_d$		
100.0%	maximum	33,000
99.5%		33,000
97.5%		32,350
90.0%		17,000
75.0%	quartile	8,650
50.0%	median	3,700
25.0%	quartile	1,100
10.0%		158
2.5%		100.5
0.5%		100
0.0%	minimum	100
Descriptive Statistics		
Mean		6047.3171
Std Dev		6971.3327
Std Err Mean		1088.7393
Upper 95% Mean		8247.7412
Lower 95% Mean		3,846.893
N		41
Variance		48599480
Skewness		1.9704897
Kurtosis		4.688515
CV		115.27976
N Missing		0

Table 19 provides a goodness-of-fit for the pH≤7.0 Pu K_d data set: lower the goodness-of-fit value, the better the model fit. The table provides a listing from best to worst. Three global metrics for good fit were used. The top three distributions each are best on one of three global goodness-of-fit metrics. The Weibull, Generalized Gamma, Loglogistic, and Lognormal have been commonly among the better models.

Table 19. Goodness-of-fit of distribution models for the Pu K_d data set for ≤pH 7.0.

Distribution	AICc	-2Loglikelihood	BIC
Weibull	797.51453	793.19874	800.62588
Exponential	798.10690	796.00434	799.71791
Generalized Gamma	799.75680	793.10815	804.24887
Lognormal	802.73341	798.41762	805.84477
Log Generalized Gamma	802.82501	796.17636	807.31708
Loglogistic	804.00174	799.68595	807.11309
Frechet	814.22946	809.91367	817.34081
LEV	823.67835	819.36256	826.78970
Logistic	838.55733	834.24154	841.66868
Normal	845.32041	841.00462	848.43177
SEV	872.39809	868.08231	875.50945

[a] AIC: Akaike information criterion; BIC: Schwartz's Bayesian information criterion; -2 log likelihood: -2 times the natural log of the likelihood evaluated with the best-fit estimates of the parameters

The distribution model fits for the sediment Pu K_d data of pH ≤7.0 are presented in Figure 6. The lognormal clearly does not fit as well as the Weibull model, with many of the lower and mid-range K_d values not falling on the lines (Figure 6). The extended generalized gamma models the data well, however, as noted earlier, it is a more complicated model, requiring additional fitting parameters. In fact, it is a special case of the Weibull model. With the extra fitting parameter the extended generalized gamma model does an excellent job of fitting the data.

Weibull Fits: Left (quantile plot: log scale on x-axis) and Right (nonparmetric plot)
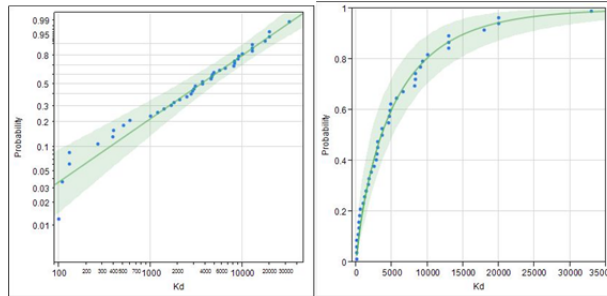
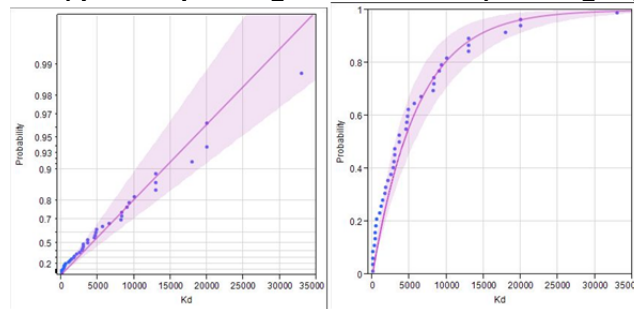**Lognormal Fits: Left (quantile plot: log scale on x-axis) and Right (nonparmetric plot)**
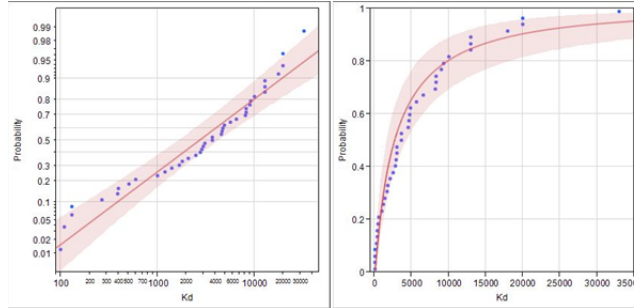
Exponential Fits: Left (quantile plot: log scale on x-axis) and Right (nonparmetric plot)

Extended Generalized Gamma Fits: Left (quantile plot: log scale on x-axis) and Right (nonparmetric plot)
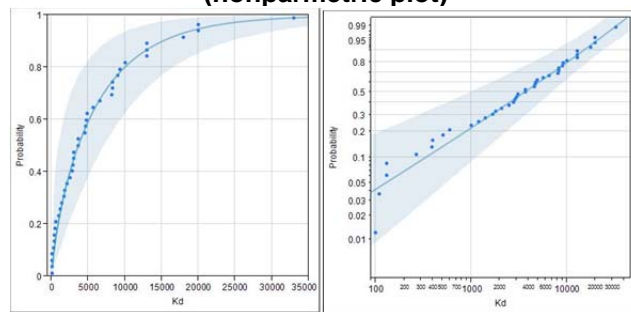

Figure 6. Weibull, lognomal Exponential and Extended Generalized Gamma model fits to the Pu K$_d$ data of pH ≤7.

4.6.4 Subsets of the Pu K_d Data Set based on pH and Sediment Texture

Additional statistical analyses were conducted with just the sandy sediments (n = 33) and just the clayey sediments (n = 31) for pH >7 and ≤7. Distribution quantile plots were drawn, AIC, -2loglikelihood, and BIC model fits were conducted to the dozen or so distribution models (Weibull, lognomal, Frechet, normal, etc.). Generally, the results are presented in Appendix A and Table 20. The Pu K_d ranges did not decrease greatly by categorizing the K_d by sediment type and pH (e.g., Clay/≤pH7, Clay >pH 7, etc…) and perhaps equally important is that the types of distribution models did not change greatly either. For this reason, statistics based on all soil types, the most robust data set, were used to develop the recommended model input parameters.

The mean Pu K_d value in each of these categories ranged from 3,830 mL/g (Sandy sediment/pH ≤7) to 13,058 mL/g (Clayey sediment/pH >7), and as such may represent the best estimate for a K_d value for these conditions (Table 20).

Table 20. Quantile and statistical analysis of sediment Pu K_d values in entire data set, sandy sediment, and clayey sediments.

Quantile		All soil All pH	All soil pH>7.0	All Soil pH≤7.0	Sand pH >7.0	Sand pH ≤7.0	Clay pH >7.0	Clay pH ≤7.0
100.0%	Max	50,000	50,000	33,000	20,000	20,000	50,000	33,000
99.5%		50,000	50,000	33,000	20,000	20,000	50,000	33,000
97.5%		44,800	50,000	32,350	20,000	20,000	50,000	33,000
90.0%		20,000	37,500	17,000	20,000	12,980	45,200	22,500
75.0%	quartile	13,000	20,000	8,650	20,000	4,850	33,000	13,000
50.0%	median	3,700	5,950	3,700	20,000	1,800	3,500	8,600
25.0%	quartile	1,250	1,300	1,100	1,545	395	1,300	3,925
10.0%		282	415	158	210	122	576	1,770
2.5%		106.5	210	100.5	210	100	540	1,000
0.5%		100	210	100	210	100	540	1,000
0.0%	Min	100	210	100	210	100	540	1,000
Statistic								
Mean		8560	12852	6047	12511	3830	13056	9513
Std Dev		10824	14526	6971	9258	5428	17249	7839
Std Err Mean		1343	2965	1089	3086	1086	4454	1960
Upper 95% Mean		11242	18985	8248	19628	6070	22608	13690
Lower 95% Mean		5878	6718	3847	5395	1589	3504	5335
N		65	24	41	9	25	15	16

4.6.5 Input Weibull Distribution Values

Table 21 and Table 22 contain input values for Weibull distributions for soil Pu K_d values and zero-inflated Weibull distributions for cement iodine K_d values. These values are for young and middle aged, oxidized cementitious materials.

Table 21. Parametric Estimate for GoldSim Calculated from Statistical Modeling of Weibull Distributions for Pu K_d Values.

Distribution	Minimum[a]	Weibull Slope	Mean-Minimum
Sand/all pH	100	0.555	6702
Sand/pH >7	210	0.499	18,234
Sand/pH≤7	100	0.560	4,096
Clay/all pH	540	0.696	11,021
Clay/pH ≤7[b]	0	1.000	9,512
Clay/pH >7	540	0.485	14,620
[a] Minimum is the statistically the best fitted value.			
[b] The distribution for the Clay/pH≤7 was also very well described as an exponential distribution with alpha (the mean) equal to 9,512. Either distribution is equally good for describing Pu K_d values under these pH conditions.			

Table 22. Input GoldSim Parametric Estimates for the Zero-Inflated Weibull Distributions for Cement Iodine K_d Values.

Distribution	Probability K_d = zero	Probability K_d = Weibull distribution	Minimum	Weibull Slope	Mean-minimum
Iodine in cement	0.25	0.75	0.0	1.377	1.596
Zero-inflated Weibull can be implemented in GoldSim by using the Discrete Distribution model to first separate whether the K_d is part of the 0 mL/g population or part of the non-zero Weibull population. An if/then statement can be used to send the non-zero data to a Weibull distribution.					

4.6.6 Recommended Values for Performance Assessments

Based on the recommendation in Kaplan (2010), the **best estimate** for a Pu K_d value in sandy sediments was 290 mL/g and in clayey sediments was 5950 mL/g. Using the pH≤7 data, the 290 mL/g sand K_d value would fall between the 10-25 percentile range (Table 20). Similarly, the 5950 mL/g clay K_d value would fall in the 25-50 percentile quantile.

Recently, and not reflected in the data set presented in Table 12, was a series of studies conducted in lysimeters on the SRS (Demirkanli et al., 2008, 2009; Demirkanli et al., 2007; Kaplan et al., 2006; Kaplan et al., 2010; Kaplan et al., 2007). These experiments reflect a higher-pedigree measurement of how Pu would behave under SRS conditions than in a short-term laboratory batch setting. In this field experiment, which lasted 11 years, Pu of varying

oxidation state (Pu(III), Pu(IV), and Pu(VI)), moved very little when exposed to natural rainfall conditions; the Pu moved through the sediment at an overall rate of <4cm/11 yr. A kinetic and solubility model (the model used 4 input values to describe Pu geochemistry, instead of a single Pu K_d value) was used to describe transport through these field lysimeters, but the single best K_d value was ~1800 mL/g ((Demirkanli et al., 2009). To date this is our best experimental estimate of a single sediment Pu(IV) K_d value. However, this lysimeter sediment contained more clay-size particles, than what is typically consider a "sandy sediment" on the SRS, thus biasing the K_d higher than expected for a sandy sediment.

It is suggested that the best-estimate for Pu K_d values in sandy sediment be increased from 290 to 650 mL/g because: 1) recent lysimeter data indicate that the experimental best estimate K_d value is in fact much closer to 1800 mL/g, and 2) quantile data indicate that the 290 mL/g data is in the lower quantiles and while conservative, may not represent a best-estimate.

Presently, there is only an empirical approach in the PA to alter K_d values to account for the impact of cementitious leachate chemistry; it is through the "cementitious leachate impact factor" (Table 2 in Kaplan 2010). This multiplier or factor can either increase K_d values, as is the case for Pu (x2) and Sr (x3), or decrease K_d values, as is the case with I (x0.1) K_d values, or have no impact on K_d values, as is the case for Cs (x1). The influence depends on chemical considerations. In the case of Pu, the presence of the cementitious leachate promotes precipitation, whereas with iodine, it promotes anion (OH^-) competition. The cementitious leachate impact factor for Pu is "2" and for I, it is "0.1."

Prikyrl and Pickett (2007) recommended a Pu K_d value for aquifer sediment K_d of 250 mL/g. Their recommendation was based on similar data as presented in Kaplan (2006; 2010), which had recommended best estimate Pu K_d values of 290 mL/g. The Pu K_d dataset in Table 12 includes all the Pu K_d data considered by Prikyrl and Pickett (2007) except this report did not include data from Prout (1958) because he used a Pu-soil contact time of only 1 day and used distilled water (which is too unlike groundwater), and did not use the data from Hoeffner (1985) because the oxidation state of the Pu was not verified.

The recommended input for the Weibull distribution for the Pu K_d values are presented in Table 23, those for the Zero-inflated Weibull distribution for cement iodine K_d values are presented in Table 22.

Table 23. Recommended Parametric Estimate for Weibull Distributions for Pu K_d Values

Distribution	Minimum[a]	Weibull Slope	Mean-Minimum
Sand/pH≤7	100	0.56	650
Clay/pH ≤7	100	0.56	5950

5.0 CONCLUSIONS

This report contains results from two tasks. The first task measured Cs, Sr, I, and Eu K_d values with simulated saltstone. The second task consisted of a critical literature review and statistical analysis of soil Pu K_d values.   For both tasks the statistical range and distribution were determined to assist stochastic modelers in site wide PA analyses.

Saltstone K_d Task – The objective of the saltstone K_d variability project was to determine the range and distribution of cesium, strontium, iodine and europium K_d values in saltstone. The scope of this study did not include understanding saltstone sorption mechanisms responsible for increasing or decreasing sorption. Cs, Sr, and I K_d values were measured from a wide range of formulations of 22 archived saltstone materials (measured in triplicate). Eu K_d values could not be measured because Eu precipitated or sorbed to glassware during the experiment. The following K_d ranges, means, and standard deviations were obtained:

- saltstone triplicate Cs K_d values ranged from 5 to 436 mL/g (mean K_d = 20 ± 15 mL/g for <60 °C samples; mean K_d = 289 ± 115 mL/g for 60 °C samples),
- saltstone triplicate Sr K_d values ranged from 122 to 6,938 mL/g (mean K_d = 528 ± 242 mL/g for <60 °C samples; mean K_d = 3383 ± 2401 mL/g for 60 °C samples)
- saltstone triplicate I K_d values ranged from -1.5 to 2.9 mL/g (mean K_d = 1.07 ± 0.97 mL/g for all samples)

The distribution of saltstone K_d values were very wide, capturing the wide array of formulations and temperature curing conditions represented in the samples.

This work suggests keeping the present method of calculating K_d value ranges for stochastic models:

$$\text{"Min"} = K_d - (1.5 * 0.5 * K_d) = 0.25 * K_d$$
$$\text{"Max"} = K_d + (1.5 * 0.5 * K_d) = 1.75 * K_d$$

This range is not as large as identified experimentally. It is possible that the experimental conditions selected are not in fact those that may prevail in the field. Furthermore, only a small number of samples were analyzed. Two types of distributions were selected for the cementitious materials. Lognormal is used for the cations (Cs, Sr etc…) and the zero-inflated Weibull for the anions that used K_d values including K_d = 0 (e.g. I). The Weibull and lognormal are very common distributions that are available in the GoldSim software presently used on the SRS for stochastic modeling for various PAs.

An unrelated and unexpected result from this research was that Cs and Sr K_d values were consistently much greater than expected, especially when the samples were cured at a temperature of at least 60 °C. This study was not designed to evaluate temperature effects on sorption and as such more research is necessary to confirm these findings. Regarding this latter

finding, more research is needed to validate this observation and understand the mechanism as knowledge on how curing profiles affect K_d is relevant to the PA and could lead to saltstone formulations that have improved performance properties. It is possible that Cs and Sr K_d variance could be greatly reduced through accounting for temperature. Stated differently, it may be necessary to measure saltstone K_d values with materials that have been temperature cured in a manner similar as the Saltstone Facility.

Soil Pu K_d Task – The range and distribution of plutonium K_d values in soils is not known. 65 SRS sediment Pu-K_d values were critically reviewed, tabulated, and then statistically analyzed to identify their range and distributions, similar to what was done with the saltstone K_d values. Further refinement of the distributions was made based on the soil texture and soil pH range. The purpose of the Pu sediment K_d dataset was not to attempt to understand through statistics how to better understand Pu sorption to sediments or to lower Pu K_d variance. The following K_d ranges, means, and standard deviations were obtained:

- pH 4.6 to 10.47 sediment Pu K_d values ranged from 100 to 50,000 mL/g (mean K_d = 8,559 ± 10,823 mL/g; to simulate a plume moving through all pH conditions),
- pH 4.6 to 7.0 sediment Pu K_d values ranged from 100-33,000 mL/g (mean = 6,047 ± 6,971 mL/g ; to simulate a plume moving through far-field conditions),
- pH 7.01 to 10.47 sediment Pu K_d values ranged from 210 – 50,000 mL/g (mean = 12,851 ± 14,525 mL/g; to simulate a plume moving through a basic cementitious plume conditions), and

The Weibull distribution was recommended for each of the Pu sediment distributions. The large range in Pu K_d was a result of a sharp rise or drop in K_d values, consequently, if the intent is to reduce the range of K_d values, then smaller ranges of pH values are recommended. The recommended best estimate Pu K_d value for sandy sediments was increased from 290 to 650 mL/g based on long-term field lysimeter studies, and the observation that the 290 mL/g value was within the 10-25 percentile of Pu K_d values in sandy sediments.

6.0 REFERENCES

Allard, B., L. Eliasson, S. Hoglund, and K. Andersson. 1984. Sorption of Cs, I and Actinides in Concrete Systems. SKB Technical Report SKB/KBS TR-84-15, SKB, Stockholm, Sweden.

Almond, P. M., and D. I. Kaplan. 2011. Distribution Coefficients (K_d) Generated from a Core Sample Collected from the Saltstone Disposal Facility. SRNL-STI-2010-00667.

Atkins, M., and F. P. Glasser. 1992. Application of Portland Cement-Based Materials to Radioactive Waste Immobilization. Waste Management. 12:105–131.

Baes, C. F., III, and R. D. Sharp. 1981. A proposal for Estimating of Soil Leaching Constants for Use in Assessment Models.. Journal of Environmental Quality 12:17-28.

Claeskens, G, and N.L. Hjort. 2008. Model Selection and Model Averaging. Cambridge University Press. New York.

Coughtrey, P.J., D. Jackson, and M. C. Thorne. 1985. Radionuclide Distribution and Transport in Terrestrial and Aquatic Ecosystems. A Compendium of Data. A. A. Balkema, Netherlands.

Demirkanli, D. I., Molz, F. J., Kaplan, D. I., and Fjeld, R. A. (2008). A fully transient model for long-term plutonium transport in the Savannah River Site vadose zone: Root water uptake. *Vadose Zone Journal* **7**, 1099-1109.

Demirkanli, D. I., Molz, F. J., Kaplan, D. I., and Fjeld, R. A. (2009). Soil-Root Interactions Controlling Upward Plutonium Transport in Variably Saturated Soils. *Vadose Zone Journal* 8, 574-585.

Demirkanli, D. I., Molz, F. J., Kaplan, D. I., Fjeld, R. A., and Coates, J. T. (2007). Modeling plutonium transport through sediment containing plutonium sources of various oxidation states: An 11-year lysimeter study. *Abstracts of Papers of the American Chemical Society* 233.

Harbour, J. R., T. B. Edwards, E. K. Hansen, and V. J. Williams. 2007. Impact of Increased Aluminate Concentrations on Properties of Saltstone Mixes. WSRC-STI-2007-00506.

Harbour, J. R., V. J. Williams. 2008. Saltstone performance Indicator – Dynamic Young's Modulus. SRNL-STI-2008-00488.

Harbour, J. R., T. B. Edwards, and V. J. Williams. 2009. Impact of Time/Temperature Curing Conditions and Aluminate Concentration on Saltstone Properties. SRNL-STI-2009-00184.

Hoeffner, S.L. 1985. Radionuclide Sorption on Savannah River Plant Burial Ground Soil—A Summary and Interpretation of Laboratory Data. DP–1702. Aiken, South Carolina: E.I. du Pont de Nemours and Company, Savannah River Laboratory.

Hoglund, S., L. Eliasson, B. Allard, K. Andersson, and B. Torstenfelt. 1985. Sorption of some Fission Products and Actinides in Concrete Systems. Mat. Res. Soc. Symp. Proc. 50:683-690.

Kaplan, D. I., D. I. Demirkanli, L. Gumapas, B. A. Powell, R. A. Fjeld, F. J. Molz, S. M. Serkiz 2006. 11-Year Field Study of Pu Migration from Pu III, IV, and VI Sources. *Environmental Science and Technology*, 40(2): 443-448.

Kaplan, D. I. and R. J. Serne. 1998. Pertechnetate Exclusion from Sediments. Radiochim. Acta. 81: 117-124.

Kaplan, D. I., and J. T. Coates. 2007. Partitioning of Dissolved Radionuclides to Concrete under Scenarios Appropriate for Tank Closure Performance Assessments. WSRC-TR-2007-00640, Rev. 0. Washington Savannah River Company, Aiken, SC 29808.

Kaplan, D. I. (2010). "Geochemical Data Package for Performance Assessment Calculations Related to the Savannah River Site," Rep. No. SRNL-STI-2009-00473. Savannah River National Laboratory, Aiken, SC.

Kaplan, D. I., D. I. Demirkanli, L. Gumapas, B. A. Powell, R. A. Fjeld, F. J. Molz, S. M. Serkiz (2006). 11-Year Field Study of Pu Migration from Pu III, IV, and VI Sources. *Environmental Science and Technology* 40, 443-448.

Kaplan, D. I., Demirkanli, D. I., Gumapas, L., Powell, B. A., Fjeld, R. A., Molz, F. J., and Serkiz, S. M. (2006). Eleven-year field study of Pu migration from PuIII, IV, and VI sources. *Environmental Science & Technology* 40, 443-448.

Kaplan, D. I., Demirkanli, D. I., Molz, F. J., Beals, D. M., Cadieux, J. R., and Halverson, J. E. (2010). Upward movement of plutonium to surface sediments during an 11-year field study. *Journal of Environmental Radioactivity* 101, 338-344.

Kaplan, D. I., Powell, B. A., Demirkanli, D. I., Fjeld, R. A., Molz, F. J., Serkiz, S. M., and Coates, J. T. (2004). Influence of oxidation states on plutonium mobility during long-term transport through an unsaturated subsurface environment. *Environmental Science & Technology* 38, 5053-5058.

Kaplan, D. I., Powell, B. A., Duff, M. C., Demirkanli, D. I., Denham, M., Fjeld, R. A., and Molz, F. J. (2007). Influence of sources on plutonium mobility and oxidation state transformations in vadose zone sediments. *Environmental Science & Technology* 41, 7417-7423.

McDowell-Boyer, L. and D. I. Kaplan. 2009. *Distribution Coefficients (K_ds), Distributions, and Cellulose Degradation Product Correction Factors for the Composite Analysis*, April, 2009, SRNL-STI-2009-00150, Savannah River National Laboratory, Aiken, SC.

Powell, B. A., R. A. Fjeld, J. T. Coates, D. I. Kaplan, and S. M. Serkiz (2002a). "Plutonium Oxidation State Geochemistry in the SRS Subsurface Environment," Rep. No. WSRC-TR-2003-00035, Rev. 0. Westinghouse Savannah River Company, Aiken, SC.

Powell, B. A., R. A. Fjeld, J. T. Coates, D. I. Kaplan, and S. M. Serkiz (2002b). "Plutonium Oxidation State Geochemistry in the SRS Subsurface Environment." Westinghouse Savannah River Company, Aiken, SC.

Powell, B. A., R. A. Fjeld, J. T. Coates, D. I. Kaplan, and S. M. Serkiz. 2002. Plutonium Oxidation State Geochemistry in the SRS Subsurface Environment: Westinghouse Savannah River Company, Aiken, SC. WSRC-TR-2003-00035, Rev. 0.

Prikryl, J. D., and D. A. Pickett. 2007. Recommended Site-Specific Sorption Coefficients for Reviewing Non-High-Level Waste Determining at the Savannah River Site and Idaho National Laboratory. U.S. Nuclear Regulatory Commission. NRC-02-07-006. Washington, DC.

Prout, W.E. 1958. Adsorption of Radioactive Wastes by Savannah River Plant Soil. Soil Science. 84:13-17.

SRNL notebook, "Grout Variability Study" WSRC-NB-2005-00039

SRNL notebook, "Grout Variability Study II" WSRC-NB-2005-00129

SRNL notebook, "Grout Variability Study # 3" WSRC-NB-2006-00025

SRNL notebook, "Grout Variability Study # 4" WSRC-NB-2006-00140

SRNL notebook, "Grout Variability Study # 5" WSRC-NB-2007-00120

SRNL notebook, "Grout Variability Study # 6" WSRC-NB-2008-00054

SRNL notebook, "Grout Variability Study # 7" WSRC-NB-2008-00114

7.0 APPENDIX A: SUPPORTING STATISTICAL ANALYSES

7.1 SALTSTONE K_d VALUES

Table 24. Saltstone Cs, Sr, and iodine K_d average and standard deviation.

| Sample ID	Cs average	Cs Stdev	Sr average	Sr stdev	I average	I stdev
GVS-93	15.0	3.8	355.0	12.5	3.0	1.9
GVS-94	22.0	2.9	472.0	58.8	0.9	1.1
GVS-100-01	21.0	1.2	809.0	178.1	1.5	0.5
GVS-100-02	208.0	73.3	1685.0	145.6	1.7	1.5
GVS-107	75.0	9.5	592.0	36.7	0.3	1.7
GVS-110	18.0	2.9	530.0	71.8	2.2	0.3
GVS-111	19.0	0.6	718.0	13.3	2.5	1.5
GVS-114	14.0	1.0	414.0	45.1	2.9	0.1
GVS-118	14.0	4.4	385.0	170.6	0.7	0.7
GVS-121	33.0	0.6	1036.0	266.2	1.4	1.8
GVS-123	23.0	5.5	798.0	223.0	0.7	1.6
TR-419	13.0	1.2	544.0	110.1	-0.1	0.8
TR-503	16.0	4.0	323.0	13.3	0.7	0.2
TR-513	22.0	1.5	397.0	88.5	-0.1	0.7
TR-517	14.0	3.0	277.0	16.6	2.1	1.7
TR-531	14.0	4.2	131.0	8.1	-0.1	0.6
TR-614	8.0	1.2	216.0	13.0	0.3	0.6
TR-616	36.0	9.1	943.0	108.6	1.1	0.7
TP-006-003	6.0	1.5	483.0	7.5	-0.2	0.7
TP-006-004	9.0	0.0	398.0	9.2	-0.1	1.2
TP-006-005	8.0	2.5	692.0	30.2	1.3	2.8

Individual data points presented in

Table 4 . K_d values (mL/g) calculated from adsorption experiments for cesium, strontium, and iodine.

Table 25. Correlation coefficients for cesium, strontium and iodine saltstone K_d values and saltstone properties.

	Cs K_d	Sr K_d	I K_d
Cs K_d	1.00		
Sr K_d	**0.95***	1.00	
I K_d	-0.07	-0.06	1.00
Water to Premix Ratio	0.16	0.16	0.39
Al. conc.	-0.15	-0.07	0.29
Max Controlled Cure Temp (°C)	**0.60***	**0.57***	-0.08
Sample Age (Years)	0.19	0.10	0.17
50% NaOH	-0.01	0.05	0.35
NaNO3	0.03	0.06	-0.20
NaNO2	0.19	0.27	0.29
NasCO3	-0.40	-0.38	-0.05
Na2SO4	-0.17	-0.10	0.18
Al-Nitrate	-0.29	-0.26	0.16
Na-Phosphate	-0.26	-0.23	-0.09

* Significant correlation at probability of obtaining a value as large or larger than 0.05 at 21 degrees of freedom, r = 0.42.

Figure 7. Histogram of Cs $\log K_d$ distribution data of 2-component normal fit demonstrating the potential presence of a second high temperature population.
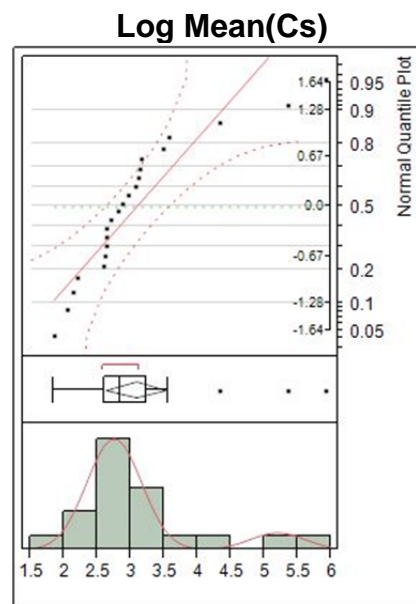

Notice the red curve 2-component normal fit to the logged mean data: it overlays the histogram (above).

Table 26. Cs K_d values (mL/g) as a function of temperature curing ranges

temperature	n	Cs K_d Median	Cs K_d Mean	Cs K_d Standard Deviation
all	22	17	45	84
60	2	289	289	115
>22	7	14	93	127
<60	20	16	20	15
22	15	18	22	15

These temperature-categories are not mutually exclusive and a K_d value may exist in more than one category.

**Iodine Distribution (with Negative Values changed to zeros)**
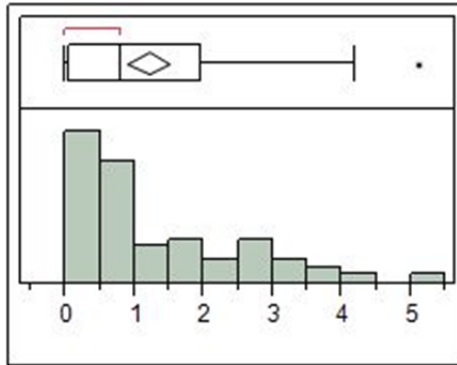
Quantiles

100.0%	maximum	5.1
99.5%		5.1
97.5%		4.515
90.0%		3.28
75.0%	quartile	1.95
50.0%	median	0.8
25.0%	quartile	0.05
10.0%		0
2.5%		0
0.5%		0
0.0%	minimum	0

Moments

Mean	1.1984615
Std Dev	1.2495615
Std Err Mean	0.154989
Upper 95% Mean	1.5080877
Lower 95% Mean	0.8888354
N	65
Variance	1.5614038
Skewness	1.1259051
Kurtosis	0.5765588
CV	104.26379

Iodine Distribution (with Negative Values changed to zeros)
Plot of the Zero-inflated Weibull fit to All of the Modified Iodine Values
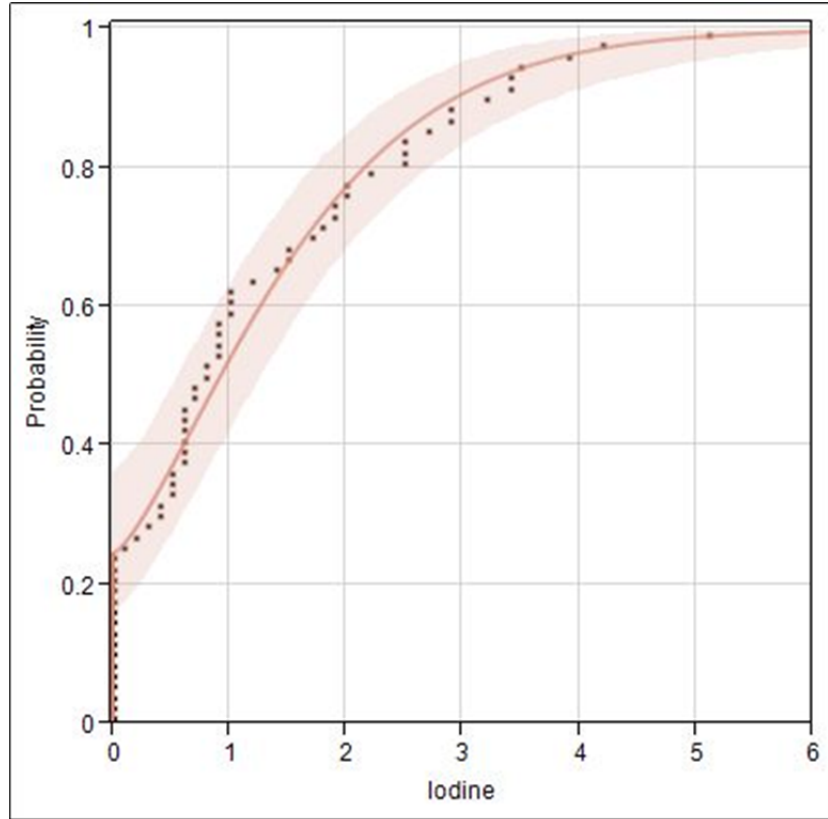
Statistics
Model Comparisons

Distribution	AICc	-2Loglikelihood	BIC
Zero Inflated Weibull	145.93402	139.54057	152.06374
Zero Inflated Lognormal	147.09249	140.69905	153.22221
Zero Inflated Loglogistic	148.90275	142.50931	155.03247
Zero Inflated Frechet	160.82707	154.43363	166.95679

Parametric Estimate - Zero Inflated Weibull

| Parameter	Estimate	Std Error	Lower 95%	Upper 95%		Criterion	
location	0.5574771	0.10965117	0.3425647	0.7723894		-2*LogLikelihood	139.54057
scale	0.7261876	0.08069536	0.5680276	0.8843476		AICc	145.93402
zero inflation	0.2461538	0.05343035	0.1566221	0.3647321		BIC	152.06374
Weibull α	1.7462612	0.19147959	1.4085555	2.1649330			
Weibull β	1.3770547	0.15302096	1.1307771	1.7604779			

Use a binary variable with probability = 0.24615 that the K_d is zero and probability = 0.75385 that the K_d cames from the Weibull distribution below.

GoldSim Parametric Estimate – Zero-Inflated Weibull

Parameter	Estimate				
minimum	0.0000				
Slope or shape	1.3770547				
Mean - minimum	1.595841				

Another interesting look at the Iodine data can be gotten if the negatives are left in the dataset.

Iodine Distribution (Including negative values)
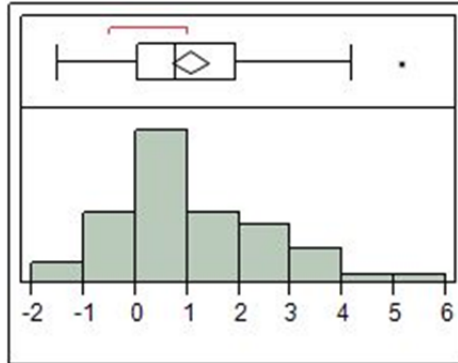
Quantiles

100.0%	maximum	5.1
99.5%		5.1
97.5%		4.515
90.0%		3.28
75.0%	quartile	1.95
50.0%	median	0.8
25.0%	quartile	0.05
10.0%		-0.64
2.5%		-1.435
0.5%		-1.5
0.0%	minimum	-1.5

Moments

Mean	1.0569231
Std Dev	1.4221429
Std Err Mean	0.1763951
Upper 95% Mean	1.4093128
Lower 95% Mean	0.7045333
N	65
Variance	2.0224904
Skewness	0.6186775
Kurtosis	0.1024054
CV	134.555

Iodine Distribution (Including negative values)
Threshold Weibull fit to All of the Unmodified Iodine Values
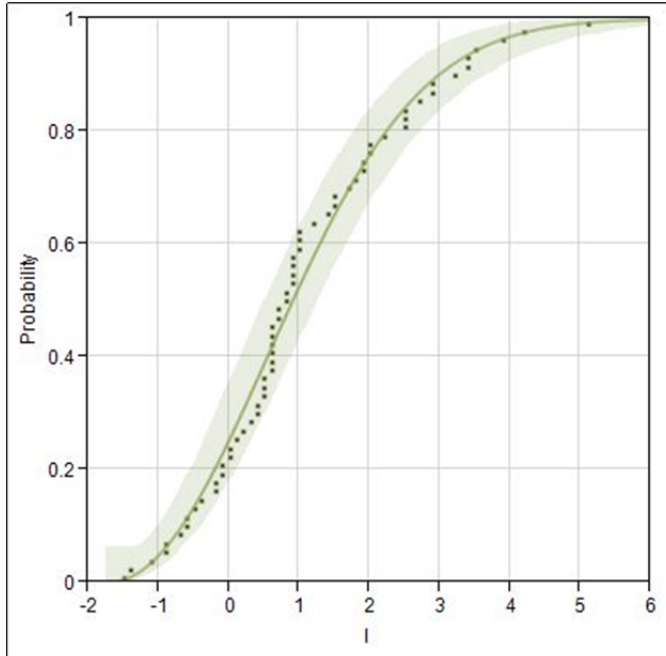
Notice that the green line has a y-intercept of about 0.25. This was about the proportion of zeros in the zero-inflated Weibull that you just looked at. As an alternative to the zero-inflated Weibull, you could just use the threshold Weibull with the parameters at the bottom of this page. Whenever you generate a negative value, you just change it to zero.

Statistics
Model Comparisons of zero-inflated Weibull fit of Iodine-Saltstone K_d dataset

Distribution	AICc	-2Loglikelihood	BIC
Threshold Weibull	229.90025	223.50681	236.02997
Threshold Lognormal	230.49271	224.09926	236.62243
Threshold Frechet	231.31360	224.92015	237.44332
Threshold Loglogistic	232.13294	225.73950	238.26266

Parametric Estimate - zero-inflated Weibull fit of Iodine-Saltstone K_d dataset

Parameter	Estimate	Std Error	Lower 95%	Upper 95%		Criterion	
location	1.151028	0.11553985	0.924574	1.377482		-2*LogLikelihood	223.50681
scale	0.481412	0.07364688	0.337067	0.625758		AICc	229.90025
threshold	-1.745199	0.25921038	-2.253242	-1.237156		BIC	236.02997
Weibull α	3.161441	0.36527241	2.520794	3.964905			
Weibull β	2.077221	0.31777502	1.598063	2.966768			

GoldSim Parametric Estimate – zero-inflated Weibull fit of Iodine-Saltstone K_d dataset

| Parameter	Estimate
minimum	-1.745199
Slope or shape	2.077221
Mean - minimum	2.800309

7.2 SOIL PLUTONIUM K$_d$ VALUES

Table 27. Statistics for relative goodness of fit model comparisons for sand with pH ≤7.

**Statistics for Relative Goodness of Fit
Model Comparisons**

Distribution	AICc	-2Loglikelihood	BIC
Threshold Weibull	438.18094	431.03809	440.69471
Threshold Loglogistic	449.67123	442.52837	452.18500
Threshold Lognormal	461.41798	454.27513	463.93175
Lognormal	461.69094	457.14548	463.58324
Weibull	462.04200	457.49654	463.93429
Loglogistic	463.47539	458.92993	465.36768
Generalized Gamma	463.90990	456.76704	466.42367
DS Lognormal	464.28834	457.14548	466.80211
DS Weibull	464.63940	457.49654	467.15317
Exponential	464.69969	462.52578	465.74466
Frechet	465.18146	460.63601	467.07376
DS Loglogistic	466.07279	458.92993	468.58656
Threshold Frechet	467.77817	460.63531	470.29194
DS Frechet	467.77886	460.63601	470.29263
Log Generalized Gamma	469.39277	462.24992	471.90654
LEV	486.18709	481.64163	488.07938
Logistic	497.31198	492.76652	499.20427
Normal	504.43632	499.89086	506.32862
SEV	520.96439	516.41894	522.85669

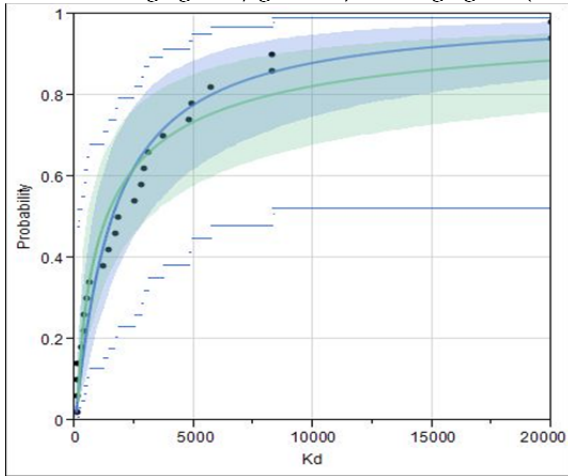Threshold Weibull (Olive) and Two-parameter Weibull (Green)
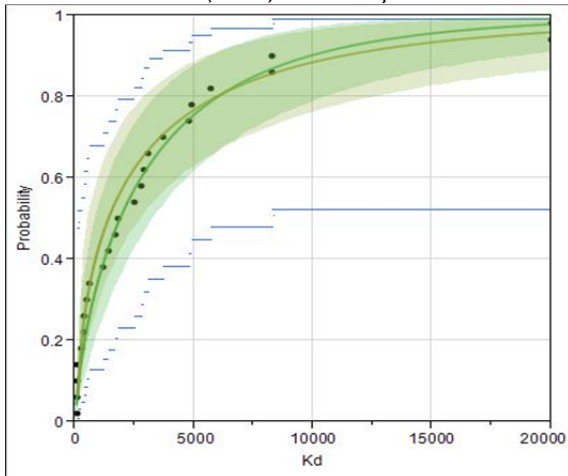
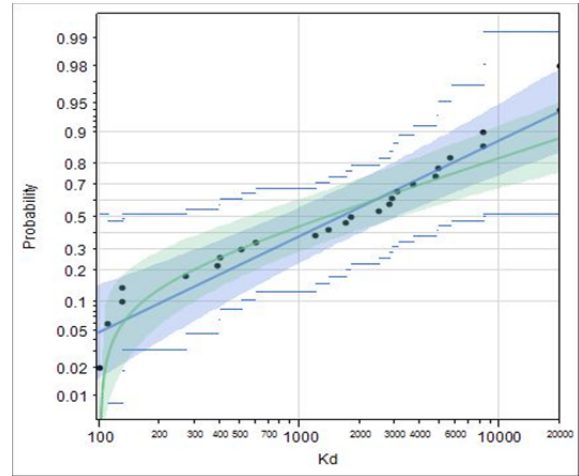Probability vs. K_d on a linear scale
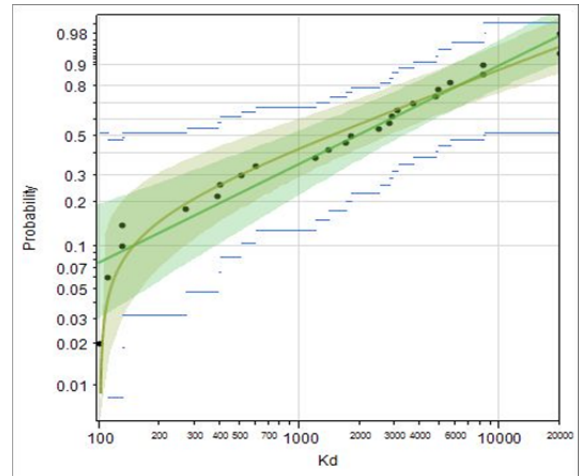
Probability vs. K_d (Weibull plots as a line)

Threshold Loglogistic (light blue) and Loglogistic (blue)

Probability vs. K_d on a linear scale

Probability vs. K_d (Loglogistic plots as a line)

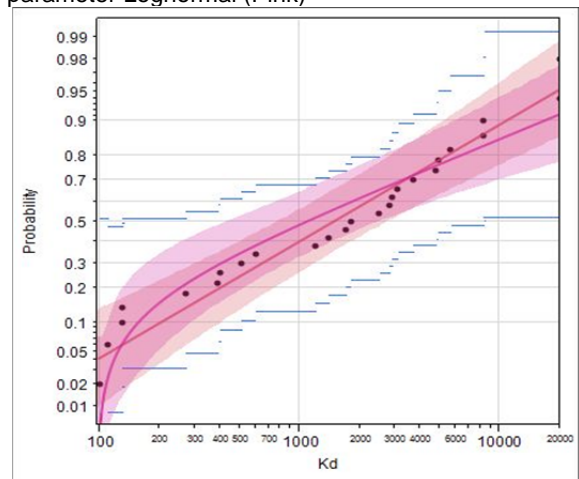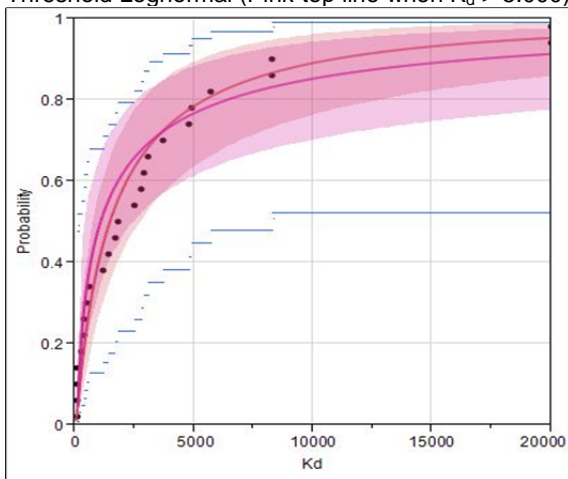Threshold Lognormal (Pink-top line when K_d > 5.000) and Two-parameter Lognormal (Pink)

Figure 8 Weibull, Loglogistic, and Lognormal fits to the sand data for pH ≤7. The left graphs plot the cumulative probability vs. K_d on a linear scale, and the graphs on the right plot K_d on a scale that should result in a straight line if the intended distribution is correct.

**Table 28.** Quantile and characterization statistics of the Sand or Clay Pu K_d values for varying pH ranges.

pH ≤7 Pu K_d data set - Sand
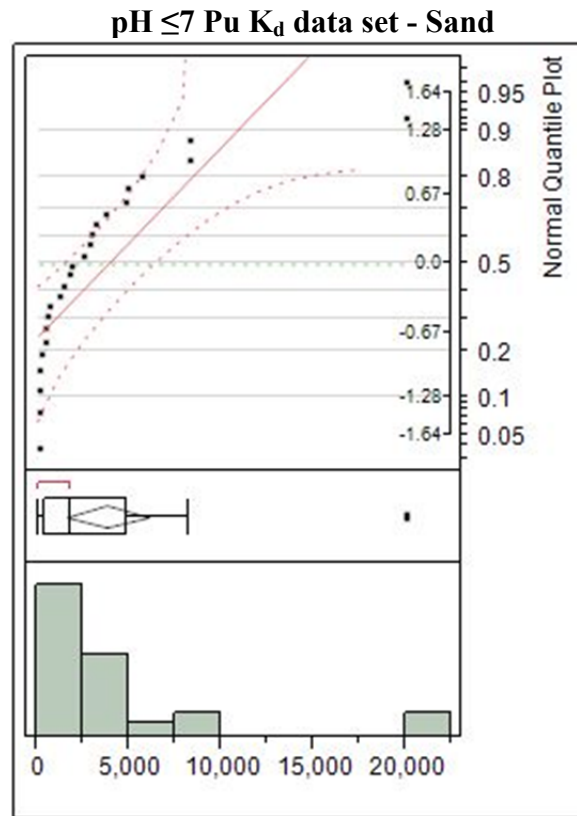
Quantiles

100.0%	maximum	20,000
99.5%		20,000
97.5%		20,000
90.0%		12,980
75.0%	quartile	4,850
50.0%	median	1,800
25.0%	quartile	395
10.0%		122
2.5%		100
0.5%		100
0.0%	minimum	100

Moments

Mean	3,829.6
Std Dev	5,427.803
Std Err Mean	1085.5606
Upper 95% Mean	6,070.087
Lower 95% Mean	1,589.113
N	25

pH >7 Pu K$_d$ Data Set - Sand
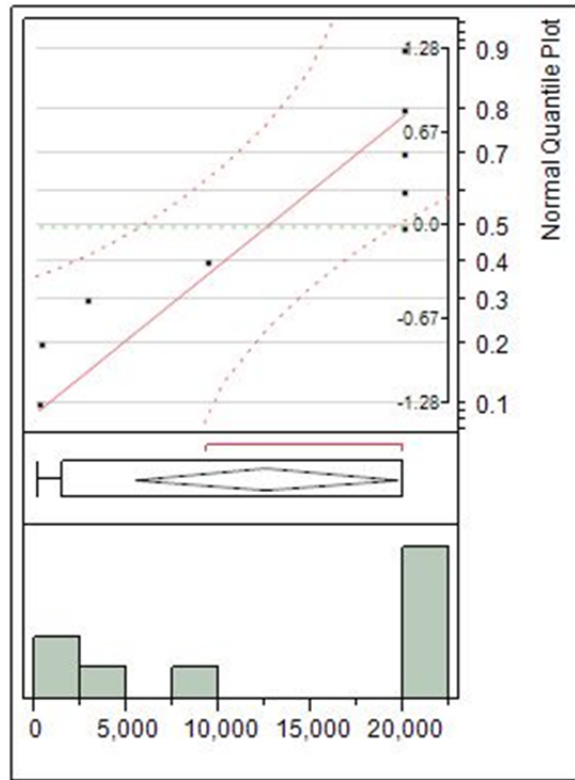
Quantiles

100.0%	maximum	20,000
99.5%		20,000
97.5%		20,000
90.0%		20,000
75.0%	quartile	20,000
50.0%	median	20,000
25.0%	quartile	1,545
10.0%		210
2.5%		210
0.5%		210
0.0%	minimum	210

Moments

Mean	12511.111
Std Dev	9258.1524
Std Err Mean	3086.0508
Upper 95% Mean	19627.557
Lower 95% Mean	5394.6652
N	9

pH ≤7 Pu K$_d$ data set - Clay
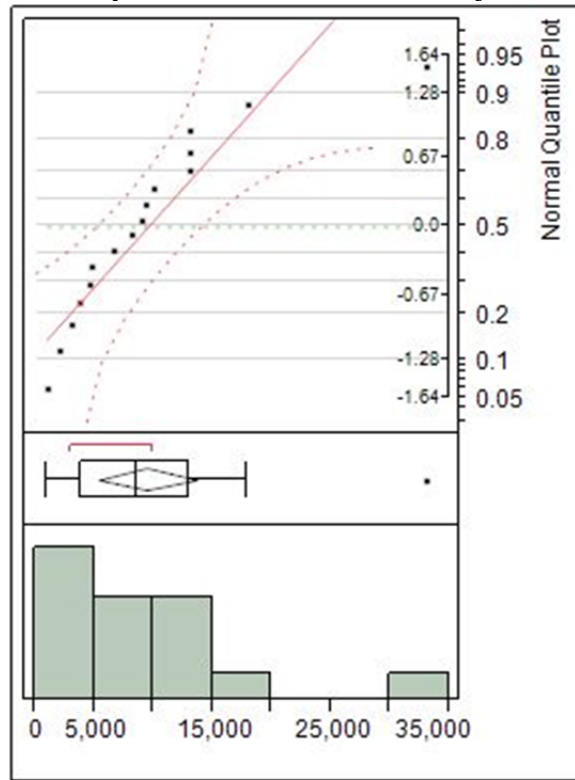
Quantiles

100.0%	maximum	33,000
99.5%		33,000
97.5%		33,000
90.0%		22,500
75.0%	quartile	13,000
50.0%	median	8,600
25.0%	quartile	3,925
10.0%		1,770
2.5%		1,000
0.5%		1,000
0.0%	minimum	1,000

Moments

Mean	9,512.5
Std Dev	7839.3771
Std Err Mean	1959.8443
Upper 95% Mean	13689.809
Lower 95% Mean	5335.1908
N	16

pH >7 Pu K_d data set - Clay
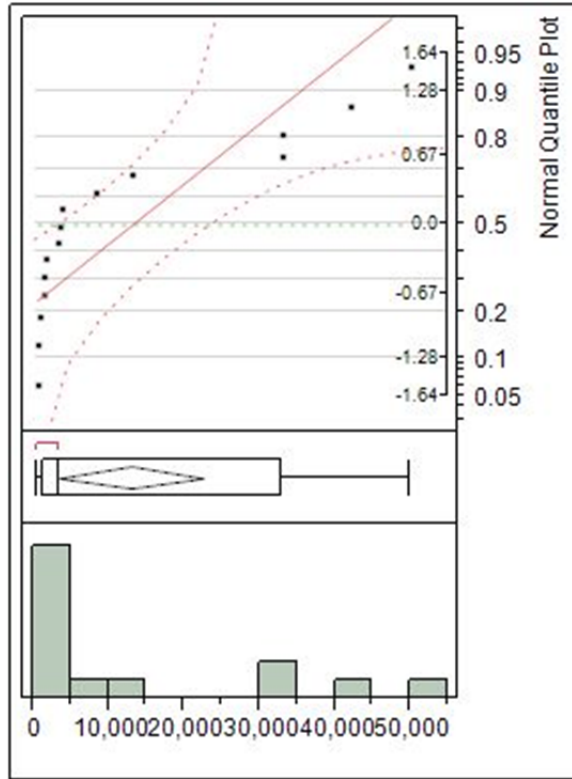
Quantiles

100.0%	maximum	50,000
99.5%		50,000
97.5%		50,000
90.0%		45,200
75.0%	quartile	33,000
50.0%	median	3,500
25.0%	quartile	1,300
10.0%		576
2.5%		540
0.5%		540
0.0%	minimum	540

Moments

Mean	13,056
Std Dev	17249.047
Std Err Mean	4453.6847
Upper 95% Mean	22608.204
Lower 95% Mean	3503.7963
N	15

8.0 APPENDIX B: Pu(IV) AND Pu(V) SORPTION EDGE AT 24 HR OR 33 DAYS (POWELL ET AL. 2002)
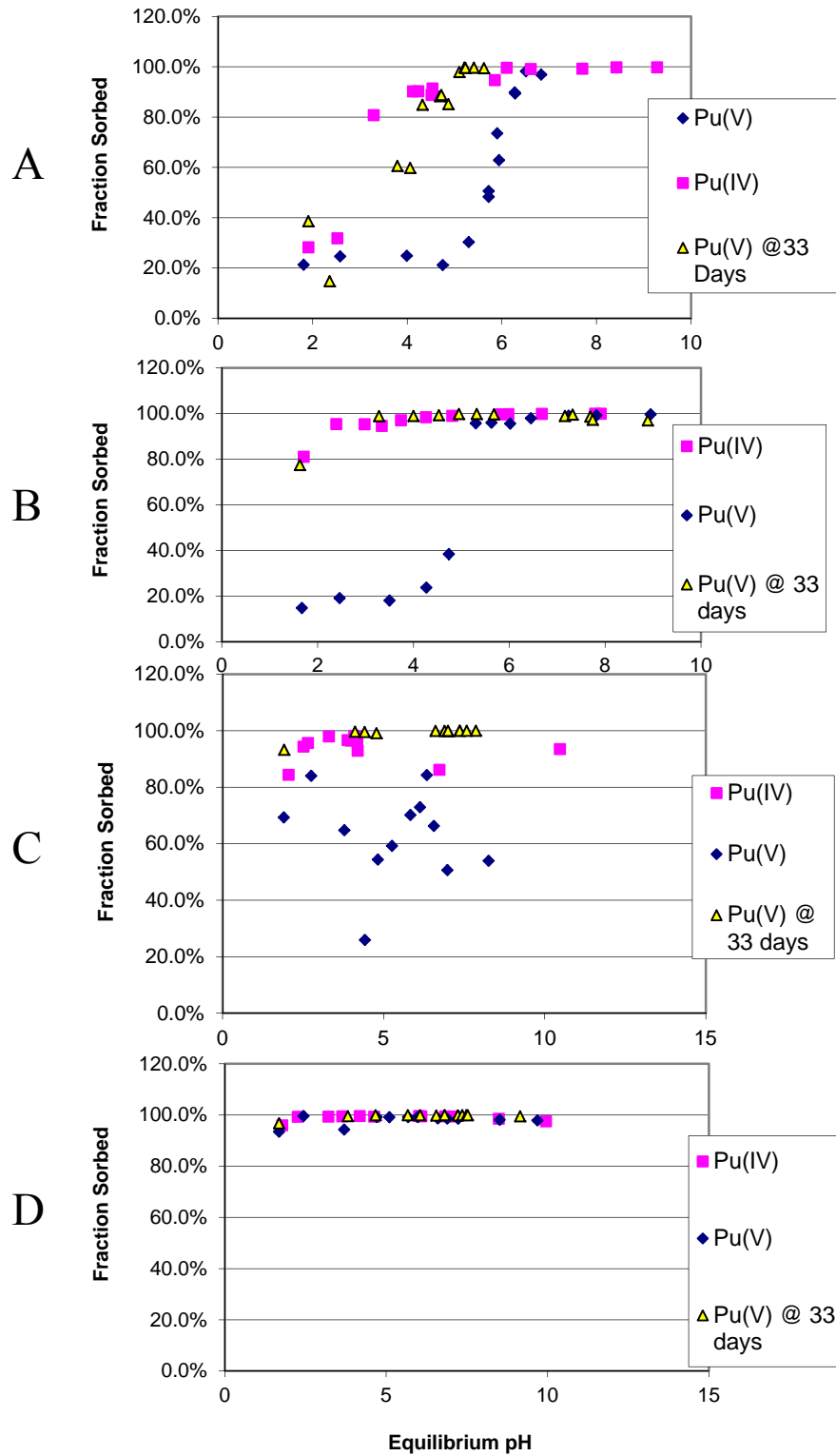
Figure 9. Pu(IV) and Pu(V) sorption edge at 24 hr or 33 days on: (A) subsurface sandy sediment, (B) subsurface clayey sediment, (C) surface sandy sediment, and (D) surface clayey sediment (Powell et al. 2002).

Distribution:

P. M. Almond, 773-43A – Rm. 227
A. B. Barnes, 999-W – Rm.336
H. H. Burns, 773-41A – Rm.214
B. T. Butcher, 773-43A – Rm.212
L. B. Collard, 773-43A – Rm.207
A. D. Cozzi, 999-W – Rm.337
D. A. Crowley, 773-43A – Rm.216
S. D. Fink, 773-A – Rm.112
G. P. Flach, 773-42A – Rm.211
B. J. Giddings, 786-5A – Rm.2
J. C. Griffin, 773-A – Rm. A-202
C. C. Herman, 999-W – Rm. 344
R. A. Hiergesell, 773-43A – Rm.218
G. K. Humphries, 705-3C – Rm.206
P. R. Jackson, 703-46A – Rm. 223
D. I. Kaplan, 773-43A – Rm.215
C. A. Langton, 777-42A – Rm.219
D. Li, 999-W – Rm.336
S. L. Marra, 773-A – Rm. A-230
F. M. Pennebaker, 773-42A – Rm.146
M. A. Phifer, 773-42A – Rm.252
S. H. Reboul, 773-A _Rm. B-132
M. M. Reigel, 999-W – Rm.404
K. A. Roberts, 773-43A – Rm.225
K. H. Rosenberger, 705-1C – Rm.33b
E. P. Shine, 702-41A – Rm. 233
F. G. Smith, III 773-42A – Rm.178
K. H. Subramanian, 766-H – Rm.2204

(1 file copy & 1 electronic copy), 773-43A – Rm.213